Antifolates as Tools for Chemical Biology

BY
LAURA E. PEDRO-ROSA
B.S. University of Puerto Rico, Rio Piedras, Puerto Rico, 2006

THESIS
Submitted as a partial fulfillment of the requirements
for the degree of Doctor of Philosophy in Chemistry
in the Graduate College of the
University of Illinois at Chicago, 2012

Chicago, Illinois

Defense Committee:

Lawrence W. Miller, Chair and Advisor
Wonhwa Cho
Brian Kay, Biology
Leslie Fung
Duncan Wardrop

This thesis is dedicated to
the memory of Max Lopez, for all his love and smile,

and

to my mother, Milagros Rosa
for her unconditional love, support and,
for teaching me to fight for what I believe in.

AKNOWLEDGEMENTS

There are many people I would like to thank that made this journey possible. First of all, I would like to thank my advisor Prof. Larry Miller for his support during these years. With his guidance I developed critical thinking skills and research skills that helped me reach to this point. Also, I would like to thank the committee members: Dr. Leslie Fung, Dr. Wonhwa Cho, Dr. Duncan Wardrop for everything taught that contributed to my growth as a chemist and researcher and special thanks to Dr. Brian Kay for his support during this process.

The Bridge to the Doctorate Fellowship, especially its directive was of great importance during my first years at UIC. I would like to especially thank Ms. Denise Yates and Dr. William Walden for their encouragement and motivation these years. Also, thanks to the Department of Chemistry staff and specially professors that contributed to my growth.

Graduate School would not be the same without my labmates, colleagues and friends. I would like to give special thanks to Nivriti Gahlaut and Harsha Rajapakse, who were with me along this journey since the beginning and special thanks to Dr. Rajashekar Reddy for all the insights in organic synthesis and everything he taught me. Also, I would like to thank the rest of my labmates Megha Rajendran, Autumn Kim, Engin Yapici and others.

Last but not least, thanks to my family for their support, especially my mother, brother and father for believing in me, to my family in Chicago that open the doors of their house and made me feel at home, thanks to Tanya Cardona, Mary Lou Lopez and Max Lopez (RIP). Thanks to the people that were there for me when I needed the most, my best friends and "brother": Kaleb Martinez and Geovannie Ojeda.

TABLE OF CONTENTS

LIST OF TABLES

TABLES **PAGE**

LIST OF FIGURES

LIST OF ABBREVIATIONS

AMP	Ampicillin
BSA	Bovine serum albumin
CAM	Chloramphenicol
CH3CN	Acetonitrile
CID	Chemical inducer of dimerization
cs124	Carbostyril 124
DBU	1,8-Diazabicyclo[5.4.0]undec-7-ene
DCM	Dichloromethane
DHF	Dihydrofolic acid
DHFR	Dihydrofolate Reductase
DHFR-TS	Dihydrofolate Reductase-Thymidilate synthase
DIPEA	Ethyldiisopropylamine
DMAP	4-Dimethylaminopyridine
DMF	Dimethylformamide
DMSO	Dimethylsulfoxide
DNA	Deoxyribonucleic acid
dTMP	Deoxythymidine monophosphate
DTPA	Diethylenetriaminepentaacetic acid
DTT	dithiothreitol
dUMP	Deoxyuridine monophosphate
EDCI	1-ethyl-3-(3-dimethylaminopropyl) carbodiimide hydrochloride
eDHFR	*E. coli* DHFR

EDTA	Ethylenediaminetetraacetic acid
Et_3N	Triethylamine
EtOH	Ethanol
FRET	Föster resonance energy transfer
g	Grams
GFP	Green fluorescent protein
GPCR	G-protein couple receptor
HBTU	O-Benzotriazole-N,N,N',N'-tetramethyl-uronium-hexafluoro-phosphate
HCl	Hydrochloric acid
HOBt	N-Hydroxybenzotriazole
HPLC	High performance liquid chormatography
HTS	High throughput screening
IPTG	Isopropyl β-D-1-thiogalactopyranoside
K_2HPO_4	Potassium phosphate
KCl	Potassium chloride
KH_2PO_4	Monobasic potassium phosphate
LB	Luria Bertani
LC	Lanthanide complex
LRET	Luminescent resonance energy tranfer
$MgSO_4$	Magnesium sulfate
MIC	Minimal inhibitory concentration
MOM-Cl	Chloromethyl methyl ether

MTX	Methotrexate
NADPH	Nicotinamide adenine dinucleotide phosphate
NaOEt	Sodiumethoxide
NaOH	Sodium hydroxide
NaOMe	Sodium methoxide
OD	Optical density
PBr_3	Phosphorus tribromide
pcDHFR	Pneumocystis carinii DHFR
pfDHFR	*Plasmodium falciparum* DHFR
PMSF	Phenylmethanesulfonylfluoride
POI	Protein of interest
TBS	Tris buffered saline
TEA	Triethylamine
TES	2-[[1,3-dihydroxy-2-(hydroxymethyl)propan-2-yl]amino]ethanesulfonic acid
THF	Tetrahydrofolic acid
TMP	Trimethoprim
TR-FRET	Time resolved foster resonance energy transfer
TTHA	Triethylenetetraminehexaacetic acid

SUMMARY

Chemical biology aims to answer fundamental biological questions by leveraging the knowledge and techniques of chemistry. Elements of protein engineering, molecular biology and, especially, synthetic organic chemistry are applied to develop reagents or methods that can be used to perturb or otherwise modulate biomolecular function. Pairs of small molecule ligands and receptor proteins that associate to the exclusion of all other environmental components within a given system (i.e., bioorthogonal interactors) can be used as powerful tools to inhibit, activate or image proteins directly in living cells or in cell lysates. Broadly, there are two strategies for achieving bioorthogonality: 1) developing bond formation reactions that occur under physiological conditions with complete, mutual selectivity; and 2) engineering non-covalent interactions between two entities (e.g., small molecule/protein or protein/protein) such that neither entity binds to other components in the system. In the case of interactions between a small molecule and a protein, both approaches typically require that each interactor be engineered synthetically or biochemically.

The interaction between the antibiotic trimethoprim (TMP) and the enzyme dihydrofolate reductase from *Escherichia coli* (eDHFR) is bioorthogonal with respect to eukaryotic systems. TMP binds to eDHFR with high affinity (~1 nM, K_I) and selectivity, and fluorescent TMP conjugates have been used to label eDHFR fusion proteins for microscopic imaging studies in live mammalian cells and yeast cell extracts. This dissertation explores, in part, the development of new chemical biology tools that leverage the interaction between selective DHFR inhibitors (antifolates) and various forms of DHFR from pathogenic organisms including *Plasmodium falciparum* and *Pneumosystis carinii*.

Three major topics are presented in this work: 1) The biochemical evaluation of antifolate/DHFR pairs as bioorthogonal interactors, 2) the potential use of fluorescent antifolates for labeling DHFR fusion proteins in living mammalian cells; and 3) the development of quantitative affinity and inhibition assays that utilize antifolates conjugated to lanthanide complexes.

Extensive medicinal chemistry research has lead to the identification of potent and selective antifolates that target different pathogenic DHFRs. In Chapter 2 of this dissertation, the synthesis of 5'-substituted benzyl pyrimidines that can be easily conjugated to fluorophores or other useful functionalities is presented. This synthesis yielded triethyleneglycolamino derivatives of 2,4-diamino-5-(4-(3,4,5-trimethoxy)-3-ethoxybenzyl) pyrimidine (compound **1a**) 2,4-diamino-5-(3,4,-dimethoxy)-5-carboxy-1-pentynylbenzyl) pyrimidine (compound **2a**), and the ability of these compounds as well as TMP to inhibit the catalytic activity of eDHFR, rat liver DHFR, *P. falciparum* DHFR (pfDHFR) and *P. carinii* DHFR (pcDHFR) was evaluated biochemically. It was observed that the conjugable antifolates **1a** and **2a** retained high potency (sub-micromolar IC_{50}) against pfDHFR and pcDHFR, respectively, while showing minimal cross-reactivity against eDHFR or rat liver DHFR. The results suggested that pfDHFR and pcDHFR may be used in combination with their antifolate partners for protein functional studies *in vitro* or in live mammalian cells.

In Chapter 3, fluorescence microscopy was used to evaluate fluorescent conjugates of **1a** and **2a** for their ability to enter live mammalian cells and label overexpressed fusions of pfDHFR and pcDHFR, respectively. The overall goal of these experiments was to develop at least one bioorthogonal, antifolate/DHFR pair that could be used in combination with TMP/eDHFR for multicolor fluorescence imaging in cells. The fluorescein conjugate of **1a** was observed to enter

NIH3T3 cells and label an overexpressed, nucleus-localized pfDHFR fusion protein. However, overexpression of pfDHFR fusions in mammalian cells had deleterious effects on cell morphology. The fluorescein conjugate of **2a** appeared to be cell impermeable.

DHFR is a common drug target because of its role in DNA synthesis. Cancer and malaria are examples of diseases were DHFR is targeted to control or cure the disease. A second aim of this research was to develop a high throughput screen to identify possible DHFR inhibitors using time-resolved fluorescence resonance energy transfer (TR-FRET). In experiments described in Chapter 4, the antifolates methotrexate, TMP and **1a** were synthetically linked to a luminescent terbium complex that can serve as a FRET donor. Both pfDHFR and eDHFR were expressed and purifed from *E. coli* as fusions to green fluorescent protein (GFP). When the GFP-DHFR fusion protein and the antifolate-terbium complex conjugate are bound to one another, terbium-to-GFP FRET was detectable at high signal-to-background ratio by using a time-resolved luminescent plate reader. Moreover, the affinity of a TMP-terbium complex for GFP-eDHFR could be accurately measured both in buffer solutions containing purified protein and in bacterial lysates. This assay platform was leveraged to quantitatively assess inhibition of the labeled methotrexate-pfDHFR interaction with unlabeled antifolates including **1a**.

The antifolate synthesis methodologies and the quantitative TR-FRET binding and inhibition assays presented in this work have set the stage for several projects that are currently underway in the Miller laboratory. The ability to synthesize substituted benzyl pyrimidines enables the development of antifolates that exhibit a wide range of dissociation rate constants with respect to eDHFR binding. Ligand-protein dissociation has implications for single molecule imaging of labeled proteins. The TR-FRET assay platform is currently being leveraged to develop a screen for inhibitors of TMP-resistant mutants of pfDHFR, and this could be a

potentially useful tool for finding therapeutically useful compounds to treat drug resistant malaria. Relatedly, a TR-FRET assay for screening and measuring protein-protein interactions and their inhibition is being developed that leverages the ability to selectively label eDHFR with TMP-terbium complex conjugates. The nature of these projects and their relationship to the work presented here is discussed in Chapter 5.

Chapter 1

INTRODUCTION AND BACKGROUND INFORMATION

1.1 Chemical Biology Tools

1.1.1 Chemical Biology

Chemical biology aims to understand and answer fundamental biological questions by studying living systems at the molecular level with tools from biochemistry, cell biology, pharmacology and especially bioorganic chemistry (1). A major focus is the use of small molecules to perturb or otherwise modulate biological systems. These small molecules may include naturally occurring metabolites that are involved in cell signaling or synthetic drugs or natural products that are used to selectively target enzymes or receptors in cellular systems for treating diseases. This idea of using small molecules to selectively perturb the function of a particular protein within a living cell or organism has come to be known as Chemical Genetics, and it is most commonly associated with the work of Stuart Schreiber, who described a major goal of the field as `to identify a small molecule partner for every gene product (2).

Whereas purely synthetic or combinatorial approaches are powerful methods for developing proteins inhibitors and drugs, (3) chemical biologists have also utilized biochemistry, molecular biology and protein engineering to prepare selective modulators of biomolecular function. For example, selective chemical coupling reactions have been developed that can be used to couple small molecules to genetically engineered proteins. These reactions have been applied to achieve cell surface labeling in animal models or to label modified proteins inside living cells (4, 5). Synthetic proteins have also been employed to answer biological questions. For example, a partly synthetic histone has been used to study postranslational modifications (6). Thus, the combination of synthetic organic chemistry and protein design makes it possible to selectively target proteins or other biomolecules within living systems. This selective labeling in

turn makes it possible to inhibit, activate, or image the targeted entities in a way that provides unique insight into the molecular mechanisms of biological function.

1.1.2 Bioorthogonal Interactions/Reactions

Interactions or reactions that occur exclusively between two molecules within a living cell or organism are said to be bioorthogonal to that particular system. Bioorthogonality is related to the concept of drug selectivity, but they are not synonymous. For example, a competitive inhibitor may bind to a unique enzyme within a cell with complete selectivity (i.e., without binding to any other cellular components), yet the targeted enzyme will still bind to its endogenous substrate. Because biological macromolecules are all composed of the same set of monomers (amino acids, nucleic acids), complete selectivity (and thus, bioorthogonality) between, say, a small molecule ligand and a given protein is rarely achieved. Nevertheless, because bioorthogonal interacting pairs offer a means to study specific events or components (e.g proteins) of interest in living systems without perturbing the native environment, their development is a consistent goal of many chemical biology investigations (7). Broadly, there are two strategies for achieving bioorthogonality: 1) developing bond formation reactions that occur under physiological conditions with complete, mutual selectivity; and 2) engineering non-covalent interactions between two entities (e.g., small molecule/protein or protein/protein) such that neither entity binds to other components in the system. In the case of interactions between a small molecule and a protein, both approaches typically require that each interactor be engineered synthetically or biochemically.

An example of a bioorthogonal, bond-forming reaction is the modified Straudinger ligation between azides and phosphines developed by Bertozzi and co-workers. Azides are absent in biological systems and relatively small making them a powerful orthogonal reporters

(Figure 1) This reaction occurs selectively between azides and triarylphosphines yielding as final product, the formation of an intramolecular amide bond upon hydrolysis and oxidation of a phosphine. The Straudinger ligation has been used to label biomolecules in different cellular environments and also in living animals. Azides can be introduced into proteins by means of non natural amino acids and uses the cell's translational apparatus. In one example, azidohomoalanine replaced methionine in proteins expressed in methionine-deficient bacterial cell cultures, by using the methionyl-tRNA synthetase in *E. coli*. The introduction of the azides is followed by the Straudinger ligation to label selectively the azido-proteins (8-10). Cell surface glycans in living animals can be chemically modified by using the metabolism of the peracetylated unnatural sugar N-α-azidoacetylmannosamine (Ac_4ManNAz), followed by the Straudinger ligation. Ac4ManN Az is introduced to the living animal interperitoneally for several days, after which a phosphine probe is also administered to the animal interperitoneally that will label cell surface glycans in living animals.

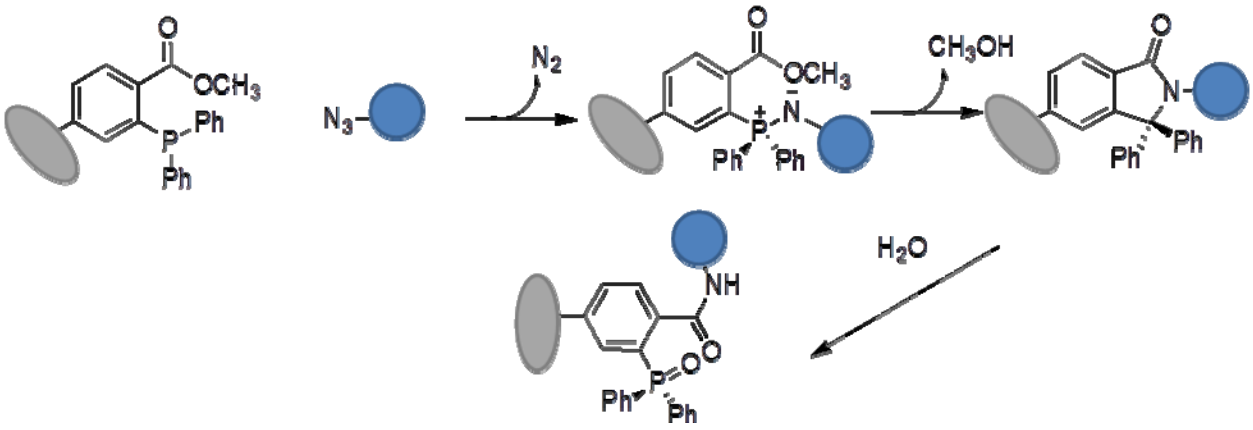

Figure 1: Schematics of a Straudinger Ligation developed by Bertozzi and coworkers (9).

One way to establish bioorthogonal interactions between a protein and a ligand is the "bump and hole" method developed by Shokat and coworkers where a kinase inhibitor interacts with a modified kinase (Figure 2). In this case, a natural kinase inhibitor was synthetically modified so that it does not bind to native kinases (by introducing a "bump"). A mutant kinase that can bind to the bumped inhibitor while retaining enzymatic activity is then expressed in cells allowing for selective inhibition of the mutant. Note that in this case, complete bioorthogonality is not achieved because the mutant kinase may still act on endogenous substrates. Nevertheless, this strategy was proven to be practically useful for overcoming the non-specificity of known kinase inhibitors, thereby allowing for selective studies of individual kinase (11). The bump-hole strategy was also exploited to develop improved chemical inducers of dimerization. Homodimeric ligands that bind to FKBP12 can be used to induce dimerization of FKBP12 fusion proteins, thereby allowing chemical control of intracellular signaling events regulated by protein-protein interactions. However, these dimerizers, *in vivo*, can interact with endogenous FKBPs triggering unwanted dimerizations. Hence, FKBP was engineered with a unique binding pocket (HOLE) that differs from endogenous FKPB and the dimerizer was modified containing bulky substituents (bump) so that interacts minimally with the endogenous FKBK and with high affinity to the engineered "hole" (7, 12). Protein engineering has also played an important role in the development of additional bioorthogonal interactions. For example, a GTPase was mutated and converted into a XTPase. This engineered protein was able to accept an unnatural substrate (13). With this strategy researchers have been able to perform genomic studies of GTPases, the largest protein superfamily.

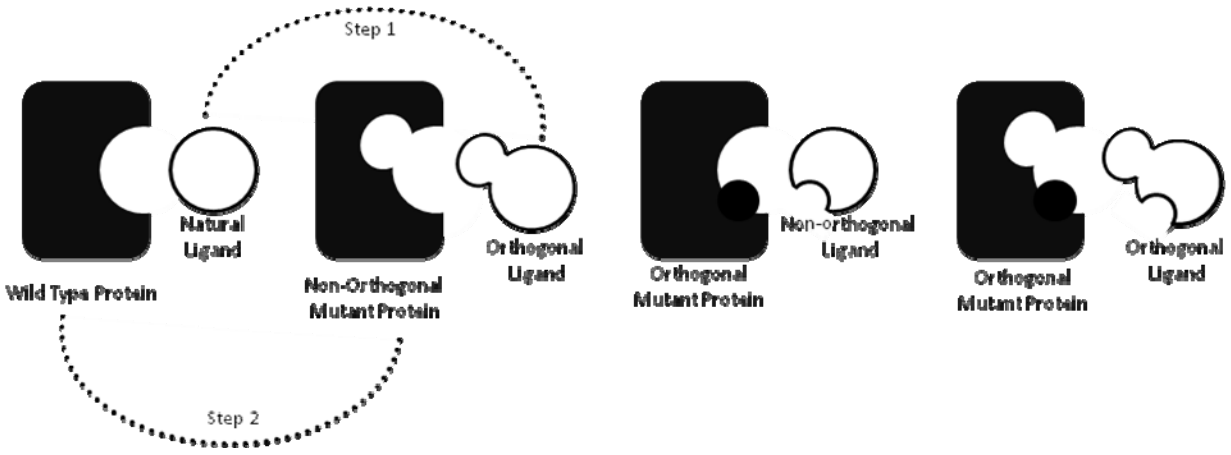

Figure 2: Schematic definition of orthogonal ligands and orthogonal proteins (7). Step 1: Substrate chemically modified into an orthogonal ligand. Step 2: Wild type protein is genetically engineered to obtain a mutant protein.

1.1.3 Chemistry in Living Systems/*In vivo* protein labeling

Another area where the ability to selectively or orthogonally label proteins or other species within living systems is useful is in the area of microscopic imaging. Genetic fusion of proteins to green fluorescent protein (GFP) or other variants has revolutionized cellular microscopy. These approaches allow the visualization of proteins in-vivo. When expressed in living cells, GFP fusions can be dynamically imaged with sub-micron resolution using fluorescence microscopy (14). While fluorescent protein fusions have proven immensely useful, the technology nevertheless has its disadvantages. For example, GFP is a barrel structure protein and the chromophore located inside the barrel structure. This structure makes it difficult to engineer GFP to be sensitive to the local chemical environment, making the development of fluorescent protein sensors problematic. Also, cellular environments are "dense/crowded", cellular components (nuclei, ribosomes, proteins, mitochondrias, etc) occupy a large area of the cellular space. The addition of large size exogenous components to the living systems may perturb the cellular functions of the proteins of interests or the function of other components in the cells. For this reason, in addition to the above mentioned examples of bioorthogonal reactions and interactions, new approaches have been developed to chemically tag proteins in living systems with small molecule fluorophores (15, 16). Because small molecules can be readily engineered synthetically to have desired photophysical or photochemical properties, selective, chemical protein labeling can overcome some of the common disadvantages associated with fluorescent proteins.

The earliest example of chemical protein labeling was the so-called FlAsH system developed by Roger Tsien. This method incorporates a tetracysteine motif into the protein of interest (POI) and uses a fluorescent biarsenical ligand (fluorescein-based, FlAsH; resorufin-

based, ReAsH) to label the POI . When the POI is expressed in living cells the biarsenical dye is added to the cells and selective labeling occurs with subnanomolar affinity when a metal-ligand bonds are formed between the tetrecysteine motif (Cys-Cys-X-X-Cys-Cys) and two arsenic atoms in the dye (17, 18). This method has been applied to study protein structure and stabilitiy (19) and also protein aggregation in Alzheimer's and Huntington's disease (20-23). While ground-breaking, the FlAsH labeling method is somewhat non-specific, with the reagents shown to non-specifically label cysteine-rich proteins (24). However, the basic stragegy wherein a recombinant protein fusion consisting of a POI fused to a receptor protein or peptide is overexpressed and labeled with a selective ligand-fluorophore conjugate has been adapted to develop other chemical protein labeling systems (Figure 3). One such system, developed by Johnson and colleagues, is a self-labeling protein technique in which a POI is fused to the human O^6-alkyl guanine transferase and labeling occur through an alkylation reaction between a fluorescent O^6-benzylguanine substrate and the transferase producing a covalently labeled POI (SNAP-Tag) (25, 26). SNAP-tag has been applied to determine protein localization, dynamics and trafficking in live cells (27-29).

A)

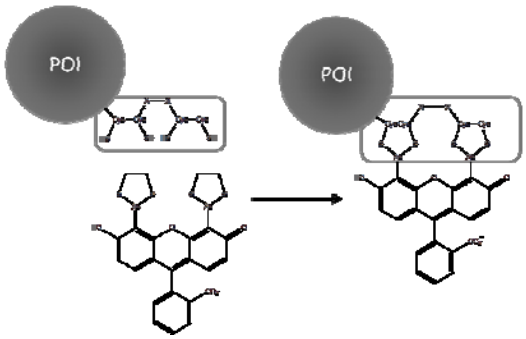

B)

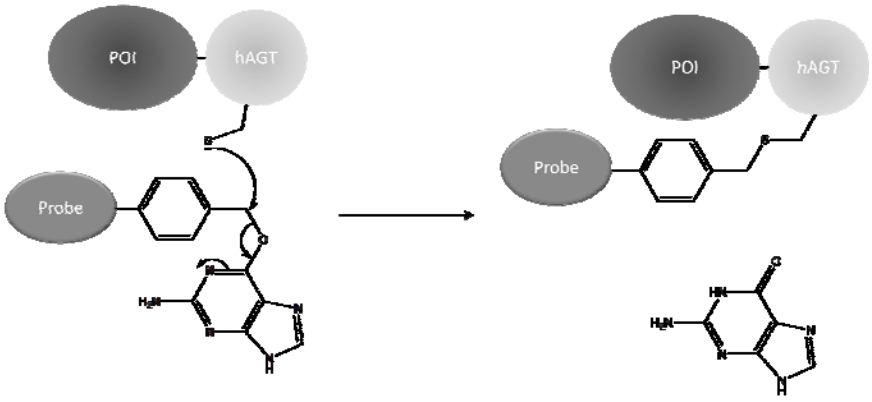

C)

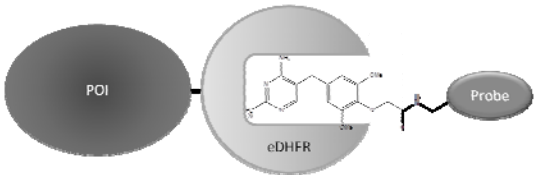

D)

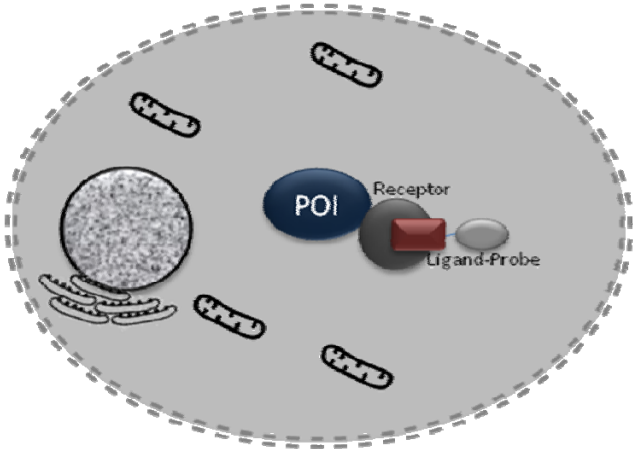

Figure 3: Chemical labeling strategies: A) FlAsH, B) SNAP-Tag, C) eDHFR-TMP, D) In-vivo protein labeling. Modified from (15)

Non-covalent chemical protein labeling approaches utilize the interaction between an engineered exogenous receptor fused to the POI with a synthetic small ligand that exhibits high affinity and specificity for the receptor. For example, Nolan and coworkers developed a selective method in which the POI is fused to an mutant version of a FK-binding protein (FKBP12(F36B)). Fusions of synthetic ligation factor (SLF) fused to fluorescein were shown to bind to the mutant FKBP with high affinity (sub-nanomolar) and selectivity. Moreover, the mutant FKBP does not interact with known components in mammalian cells (i.e., the interaction is bioorthogonal to mammalian systems (30, 31).

Of special interest is another non-covalent labeling technique developed by Cornish and coworkers, where *Escherichia coli* dihydrofolate reductase (eDHFR) is genetically linked to DNA encoding POI, and a DHFR inhibitor (antifolate) covalently coupled to a fluorophore is used to label the overexpressed protein fusion in mammalian cells. The antifolate trimethoprim (TMP) interacts weakly with mammalian enzymes (Ki >1 μM) however it strongly inhibits bacterial forms of DHFR (Ki = ~1 nM). This difference in affinities makes the TMP/eDHFR interaction bioorthogonal to mammalian systems, and TMP-fluorophore conjugates have been used to label eDHFR fusion proteins in a wide variety of wild-type mammalian cell lines (32-35). As detailed below, DHFR has been an extensively studied drug target for a variety of antimicrobial therapeutics. Consequently, there has been considerable effort in the medicinal chemistry field to develop competitive inhibitors for DHFR's from a variety of pathogenic organisms that exhibit high selectivity over mammalian DHFR as well as high potency or affinity (36-39). This work serves as the impetus for the studies presented in this dissertation, where I have sought to exploit selective antifolates and pathogenic DHFR's as bioorthogonal interaction pairs for chemical biology and biotechnology applications.

1.2 Dihydrofolate Reductase

1.2.1 DHFR Role/ Pathway

The enzyme DHFR is, in most organisms, a monomeric protein, but it can also be found as part of a complex with thymidylate synthetase. It is relatively small and its size can range from ca. 18 to 30 kDa. DHFR catalyses the reduction of dihydrofolic acid into tetrahydrofolic acid by a hydride transfer from the cofactor NADPH (Figure 4).

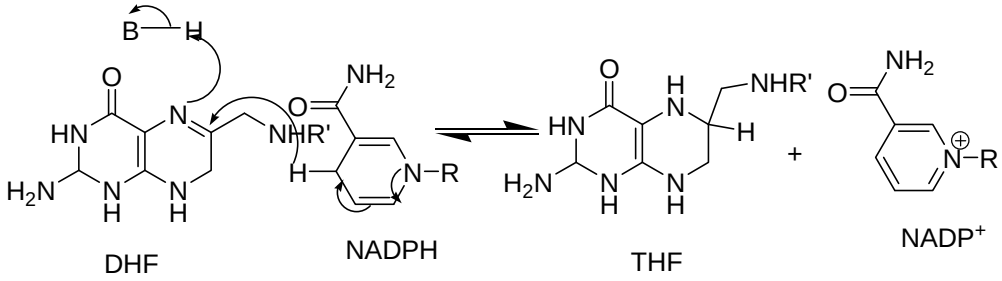

Figure 4. Dihydrofolate Reductase hydride transfer mechamism

DHFR is present in every dividing cell in every organism, but its concentration varies depending on the location (40, 41). The essential function of this enzyme is to maintain the levels of tetrahydrofolic acid in the cells. This product is an essential cofactor in the biosynthesis of thymidylate, purine nucleotides (40). Tetrahydrofolate also plays an important role in the synthesis of phenylalanine, tyrosine and tryptophan. Because of its importance DNA synthesis,

extensive research has been performed to develop selective inhibitors for the enzyme with high affinity (i.e antifolates). The development of the antifolate methotrexate, an antitumor chemotherapeutic, helped researcher identify and characterize this enzyme (42).

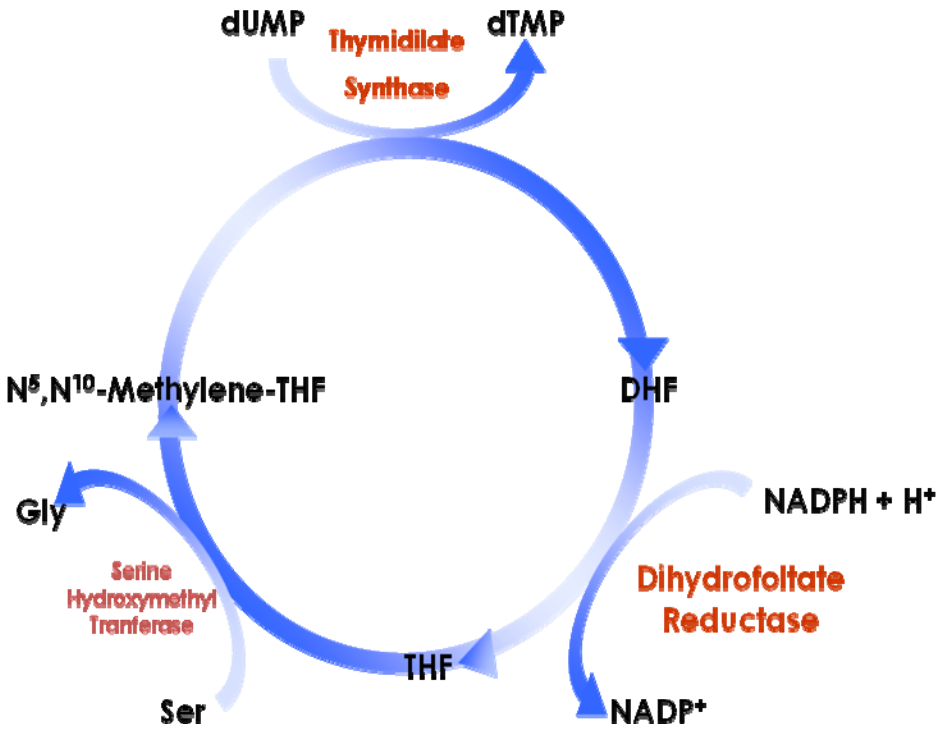

Figure 5. Conversion of dUMP to dUTP by thymidilate synthase and DHFR.

1.2.2 Antifolates development

In the 1950's while researcher where trying to find the mechanism of action of some folic acid antagonists, the enzyme dihydrofolate reductase (DHFR) was found to be the target of some of these drugs used to treat patients with leukemia (42). It was believed that leukemia was caused by a deficiency of folic acid, but treatment with folic acid increase the symptoms of the disease. Hence, researchers sought out folic acid antagonists (antifolates) to stop the effects of folic acid. The first antagonist synthesized was aminopterin (Figure 6). This compound demonstrated to be effective in the treatment of leukemia (43). Because of its effectiveness, researcher studied aminopterin's mechanism of action, finding that DHFR was the target of this compound. With this discovery, different selective folic acid antagonists (antifolates) were designed. The drugs trimethoprim (TMP) and methotrexate (MTX) were developed. Hitchings and colleagues demonstrated that TMP selectively inhibits parasitic and bacterial forms of DHFR. Also studies with MTX demonstrated higher effectiveness over aminopterin, turning MTX the drug of choice in the clinics, for treating not only leukemia but also different types of cancer.

Since the 1950's antifolates have been a common group of drugs to inhibit cell growth and proliferation. Pathogenic DHFRs have been targeted with antifolates, including those of the malarial parasite, *Plasmodium falciparum* DHFR (pfDHFR) as well as *Pneumocystis carinii* DHFR (pcDHFR), an opportunistic fungal pathogen that afflicts immune-compromized patients. Pathogens that express antifolate-resistant DHFR mutants have emerged over the past, and for this reason, the development of novel antifolates with activity against these resistant pathogens has remained in ongoing field of study in medicinal chemistry (36-39, 44).

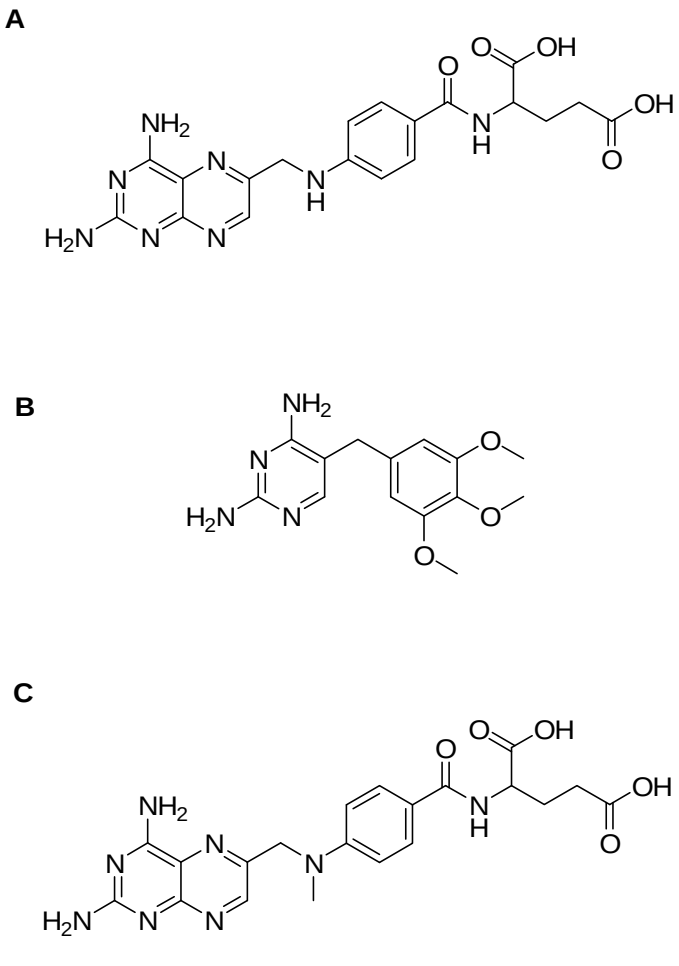

Figure 6: Antifolates. A) Aminopterin, B) Trimethoprim (TMP) C) Methotrexate (MTX)

1.2.3 *Plasmodium falciparum* DHFR

The enzyme DHFR in the organism *Plasmodium falciparum* is found as a bifunctional protein along with the enzyme thymidylate synthetase. The DHFR domain in the complex is ca. 27 kDa and it is insoluble when over expressed in *E. coli.* (45). Several studies have been performed to develop a soluble domain of the DHFR enzyme. Among the mutations, a single mutant, K27E, improves the solubility of the domain (> 13mg/ml) (46). This mutation opened a window of possibilities to study the enzyme *in vitro*.

This bifunctional DHFR-TS protein has been a common target for anti-malaria therapy. Antifolates have been used successfully to treat malaria, however resistance to trimethoprim and other drugs has emerged. Resistance to antifolate therapy has been shown, in part, to result from mutations in the DHFR domain of the DHFR-TS complex. For example, mutations at the positions C59R S109N confer resistance to both TMP and pyrimethamine, another type of antifolate (47, 48). For this reason, novel antifolates are being sought that exhibit high potency against TMP-resistant forms of pfDHFR while retaining acceptable levels of selectivity. Many discovery efforts focus on the benzyl pyrimidine scaffold represented by TMP, and a particularly potent and selective analog was developed by Yuthavong and coworkers that exhibits ca. nanomolar inhibition against pfDHFR (C59R, S108N) while exhibiting 100-fold less potency against human DHFR (39). Given the development of a soluble pfDHFR domain and suitably selective inhibitors, I sought to develop this interaction pair for studies in mammalian systems, as detailed in subsequent chapters.

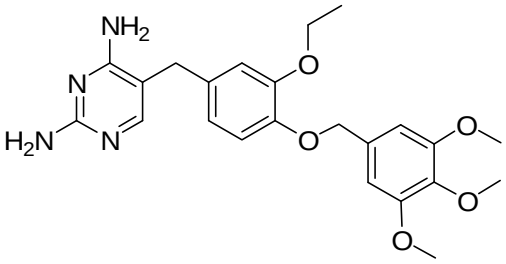

Figure 7. Compound 1. Inhibitor of *Plasmodium falciparum* DHFR.

1.2.4 *Pneumocystis carinii* DHFR

In *Pneumocystis carinii*, unlike in many other pathogenic organisms, the enzyme DHFR is found as a monomeric protein of ca. 24 KDa. This protein has been the target for treatment in immunosupressed or immunodeficient patients affected by life-threatning oportunistic fungal infection. Treatment of the infection consisted in the combination of sulfonamides and trimethoprim, or piritrexim and leucovorin but toxic and allergic side effects and low affinity of trimethroprim and low selectivity of piritrexim, have triggered the search for new therapies.

The main goal of the discovery efforts is to develop/discover new lipophilic DHFR inhibitors that combine the selectivity of TMP and the potency of piritrexim without the need of sulfa drugs or leucovorim. The focus of the discovery has been the development of 2,4-diamino-5- (substituted benzyl) pyrimidines. A potent antifolate (Figure 8) was developed by Rowosky which presented an IC_{50} of 1 nM for pcDHFR over 5000 nM for mammalian DHFR (44). Given the numerous studies on the development of these antifolates and the observed selectivity and potency of this compound, I sought to study more in depth the interaction of this compound with different DHFR, to exploit its use as bioorthogonal ligand in-vivo.

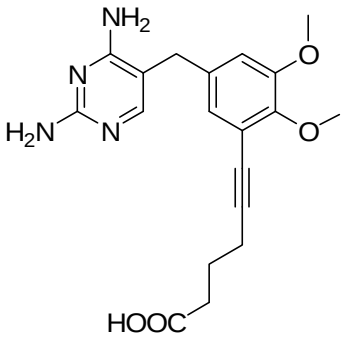

Figure 8: Compound 2. Inhibitor of *Pneumocystis carinii* DHFR

1.2.5 Importance as tools for chemical biology and biotechnology

Given the inherent selectivity of previously developed antifolates that target pathogenic organisms, and the previous successful expression of eDHFR fusion proteins in mammalian cells, it is logical to exploit this knowledge for the development of new bioorthogonal interaction partners that can be used for both live cell or *in vitro* studies of mammalian proteins. A key advantage of this strategy is that non-mammalian DHFR's should not interact with other mammalian proteins. Thus, given sufficient selectivity of the antifolate ligand, the extensive protein engineering required to achieve orthogonality in, say, the bump-hole strategy is avoided. One possible application is the development of multiple, mutually exclusive interacting ligand/receptor pairs that could be used to simultaneously label different POI's in a single cell with differently colored fluorophores. There are potentially other applications besides imaging that could be developed as well. For example, TMP and eDHFR were used to develop a novel chemical inducer of dimerizarion (CID) (49, 50). In addition to live-cell applications, the TMP/eDHFR interaction has been shown to be effective for labeling proteins for *in vitro* applications, including labeling with luminescent lanthanide complexes for studies in bacterial

lysates (51, 52) and labeling fusion proteins in yeast lysates for single molecule analysis of spliceosomes (53).

Given the importance of selective binding of antifolates to given DHFR's, a key component of these studies was the synthesis of substituted analogs of the benzyl pyrimidines, Compound 1 and Compound 2, and assessment of their relative potency against a panel of DHFR targets, including those from *P. falciparum, P. carrinii, E. coli* and mouse. Potency was evaluated by measuring relative inhibition (as *Ki*) using a standard activity assay for DHFR as well as a novel time-resolved, luminescence resonance energy transfer (LRET) assay that allowed for direct measurement of dissociation constants (K_D's). Background information on these techniques is provided in the subsequent sections.

1.3 Enzyme: Substrate Binding and Enzyme Inhibition

A straightforward way to directly compare the efficacy of enzyme inhibitors is to assess their effects on enzyme kinetics. DHFR inhibition studies are presented in chapter 2 as a means of determining the relatively selectivity and potency of a set of inhibitors for select DHFRs from various organisms. General background on enzyme kinetic analysis and inhibition is provided in this section.

1.3.1 Equilibrium binding measurements

DHFR obeys Michaelis-Menten kinetics, the assumptions of which are as follows:

- The enzyme:substrate complex (**ES**) forms rapidly upon the interaction between the enzyme and substrate.
- The enzyme and substrate react exclusively with each other, and the ES complex dissociates to obtain the product (**P**) and a free enzyme

- The reaction is observed under conditions of excess substrate, allowing the ES complex formation not to be altered by the concentration of substrate.
- The rate limiting step is the dissociation of ES to obtain free enzyme and **P** (i.e., the enzyme-catalyzed reaction is at steady state)**.**
- The reverse product formation reaction velocity is insignificant.

Based on these assumptions, a kinetic scheme for the reaction can be written as:

$$E + S \underset{k_{-1}}{\overset{k_1}{\rightleftarrows}} ES \xrightarrow{k_p} E + P\,, \qquad (1)$$

where ***E*** is the free enzyme, ***S*** is the free substrate and ***P*** is the product. ***ES*** represents the bound state of the enzyme and substrate, and k_1 and k_{-1} correspond to the kinetic association and dissociations constants respectively. k_p reperesents the kinetic constant for the conversion of bound substrate to product and its release from the enzyme.

The general expression for the velocity, or rate of this equation is:

$$v = \frac{d[P]}{dt} = k_p[ES] \qquad (2)$$

It is possible to obtain a solution for the velocity equation by assuming that [ES] maintains a steady state, that is:

$$\frac{d[ES]}{dt} = k_1[E][S] - k_{-1}[ES] - k_2[ES] = 0 \qquad (3)$$

Further derivation yields the well known Michaelis-Mented equation, that describes the initial velocity of the enzyme catalyzed reaction as a function of experimentally measurable quantites:

$$v = \frac{k_p[E]_T[S]}{K_M + [S]} = \frac{V_{max}[S]}{K_M + [S]} \qquad (4)$$

where ***v*** represents the initial velocity at a given substrate concentrations, [S], $\boldsymbol{k_p}$ represents the rate constant of the ES complex breakdown and formation of P, and $\boldsymbol{[E_T]}$ represents the total enzyme concentration. The initial velocity can be defined as , $v = k_p[ES]$. At high substrate concentrations, it is assumed that $[ES] = [E]_T$. Thus, $V_{max} = k_p[ES] = k_p[E]_T$.

K_M is the Michaelis constant, equal to $(k_{-1} + k_2)/k_1$, equal to the substrate concentration at which the reaction velocity is half-maximal. The Michaelis constant can also be expressed as:

$$K_M = \frac{k_{-1}}{k_1} + \frac{k_p}{k_1} = K_D + \frac{k_p}{k_1} \qquad (5)$$

where, K_D is the dissociation constant of the Michaelis complex when $k_p < k_{-1}$. Thus, for systems that obey Michaelis-Menten kinetics, appropriate kinetic experiments can be designed that yield information about enzyme-substrate affinity and, as shown below, enzyme-inhibitor affinity (54).

1.3.2 Enzyme inhibition

Inhibition assays make it possible to study enzymes' catalytic sites, substrate binding sites, or the kinetic mechanisms of catalyzed reactions. In the case of competitive inhibitors, where the inhibitor binds to the same site as the substrate, robust inhibition assays can allow for head-to-head comparison of relative enzyme-inhibitor affinities. Antifolates are competitive inhibitors of DHFR.

The kinetic scheme for competitive inhibition can as follows:

$$E + S \underset{k_{-1}}{\overset{k_1}{\rightleftarrows}} ES \xrightarrow{k_p} E + P \qquad (6a)$$

$$E + I \underset{k_{-2}}{\overset{k_2}{\rightleftarrows}} EI \rightarrow \text{No Reaction} \qquad (6b)$$

where, ***I*** represents the inhibitor, k_2 and k_{-2} are the association and dissociation rate constants for enzyme-inhibitor complex formation, respectively, and the other symbols are as described for equation 1. It is assumed that the enzyme and inhibitor bind reversibly and are in rapid equilibrium. Assuming that initial velocity is proportional to [ES] at steady state, the velocity in the presence of a competitive inhibitor (v_i) will approach the same V_{max} observed without inhibitor present. Similarly, the concentration of substrate required to reach half V_{max} (K_m), will increase in the presence of a competitive inhibitor ($K_{m,\,app}$) (54).

Following the same logic used to derive the Michaelis-Menten equation, an expression for the initial velocity of an enzyme catalyzed reaction in the presence of a competitive inhibitor may be derived and written as:

$$v_i = \frac{V_{max}[S]}{K_m(1+\frac{[I]}{K_I})+S}, \text{ or} \qquad (7a)$$

$$v_i = \frac{[S]}{K_{m,app}+[S]}, \qquad (7b)$$

where K_i, the inhibition constant, represents the equilibrium dissociation constant for the enzyme-inhibitor complex, ***I*** represents the inhibitor concentration, and the other terms are as defined above. Thus, by observing rates of enzyme catalyzed reactions at different substrate and/or inhibitor concentrations, useful information about enzyme-inhibitor affinity may be obtained.

Equation 7a may be rearranged to obtain another experimentally useful quantity, IC_{50}, or the concentration of inhibitor that yields $v_i = 0.5V_{max}$:

$$v_i = \frac{V_{max}[S]}{K_m(1+\frac{IC50}{K_I})+[S]} \text{ and,} \qquad (8)$$

$$IC_{50} = K_I(1 + \frac{[S]}{K_m}) \quad . \qquad (9)$$

The above-described equations serve as the basis for comparitive studies of antifolate inhibition presented in Chapter 2 (55).

1.4 Föster Resonance Energy Transfer (FRET)

Föster Resonance Energy Transfer (FRET) can be described as the non-radiative energy transfer from an excited state of a luminescent donor molecule to an acceptor molecule (not necessarily luminescent) that is in close proximity. This energy transfer occurs only if: 1) the emission spectrum of the donor overlaps with the excitation spectrum of the acceptor; 2) the dipoles of both species (i.e. donor emission dipoles and acceptor absorption dipoles) are appropriately oriented; and 3) both species are sufficiently close to one another (<10 nm). FRET is very sensitive to changes in the relative distances of donor and acceptor (10-70 Å). These changes can be observed and quantified to be used to not only measure the distance between the donor and acceptor but also to monitor relative changes in the interactions of donor- and acceptor-labeled molecules.

1.4.1 Lanthanides Complex Probes and FRET

Luminescent organic lanthanide complexes (LCs) have been widely used as donor probes in energy transfer experiments because of their unusual spectral characteristics, including multiple, narrow (<10 nm at half-maximum) emission spectra and long emission lifetimes (~ms) (29, 56-58). The narrow emission spectra make it possible to effectively separate donor emission from acceptor emission. If the acceptor is a conventional fluorescent species with ~ns emission lifetime, the donor-sensitized emission of the acceptor that is seen when FRET occurs will exhibit lifetime equal to the lanthanide donor (~ms). As the emission of lanthanides is not

technically fluorescence (singlet-singlet transition), FRET between an LC and a conventional fluorophore is sometimes referred to as luminescence resonance energy transfer, or LRET. By using time-resolved detection, where a short pulse of light excites the sample, and a brief delay (~μs) is implemented between excitation and detection, it is possible to temporally separate LRET-sensitized acceptor emission from directly excited acceptor emission. Thus, LRET-based assays of molecular interactions, where one species is labeled with a lanthanide complex (usually terbium or europium) and another with a conventional, short-lifetime fluorophore, are highly sensitive because the sensitized acceptor emission (indicating interaction) can be detected at high signal-to-background ratio.

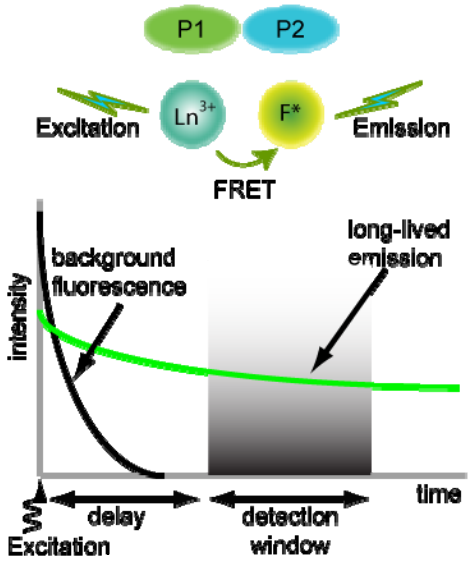

Figure 9. Time Resolved Luminescent Resonce Energy Transfer. Long lifetime, sensitized acceptor emission is detected, eliminating background autofluorescence.

As lanthanide ions are only weakly luminescent, LCs typically have three basic components that make them useful as biological probe molecules: 1) a chelating moiety; 2) a reactive functional group; and 3) an organic chromophore. The chelating moiety serves to tightly bind the lanthanide ion and shield it from the quenching effects of water and also acts as a scaffold to link chromophore and the reacting group. The reactive functionality allows for covalent conjugation or non-covalent binding to biomolecules. The organic chromophore serves as an antenna or sensitizer that absorbs excitation light (typically, 320-380 nm) and transfers the energy to the emissive level of the lanthanide. because the lanthanides inability to be excited efficiently by themselves. In these studies, we show that antifolates can be linked to a carbostyril124-sensitized, polyaminocarboxylate terbium complex. By using time-resolved LRET detection, we show that dissociation constants between antifolate-LCs and fusions of DHFR to GFP can be measured with high sensitivity and accuracy.

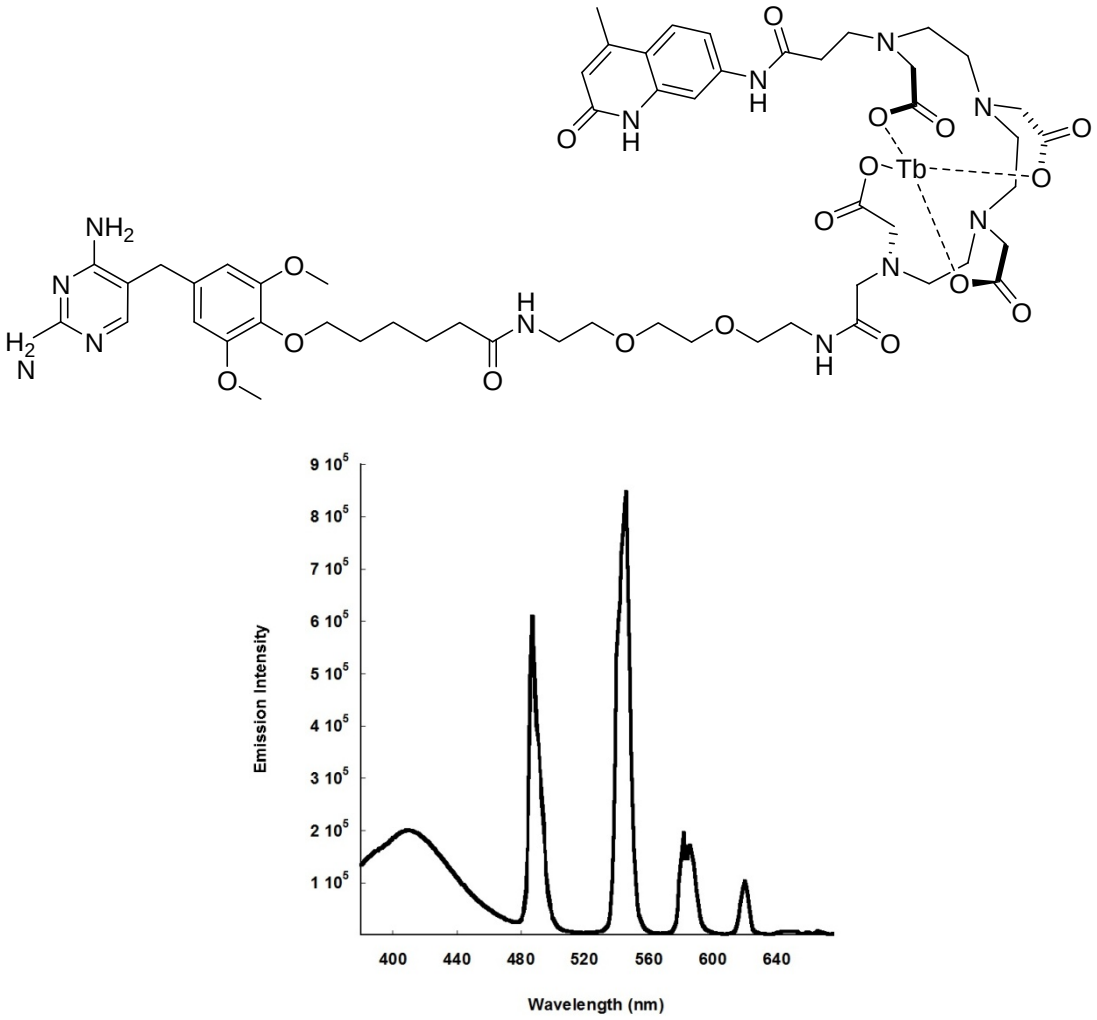

Figure 10: TMP TTHA cs124 Tb^{3+} . Tb^{3+} sensitized emission spectra

Bioorthogonal ligand-receptor interactions can be exploited to develop useful tools that can be used to study protein function in living systems, assay fundamental biophysical parameters (e.g., ligand-receptor affinity) or as part of drug discovery efforts. In subsequent chapters, a comprehensive analysis of the intearaction between select antifolates and their respective DHFR targets is presented. These chapters emphasize the *in vitro* and *in vivo* characterization of ligand-receptor interactions that are putatively bioorthogonal to mammalian systems, with special interest given to the interaction of trimethoprim resistant *Plasmodium falciparum* DHFR and Compound **1** and *Pneumosystis carinii* DHFR and Compound **2**. In Chapter 3, evidence is presented showing that a fluorescent analog of Compound **1** can be used to label a pfDHFR fusion in live mammalian cells. In Chapter 4, the development of quantitative, TR-LRET assays for ligand-receptor binding is presented, and finally, in Chapter 5, a synopsis of ongoing and future work made possible by these studies is given.

Chapter 2:

SEEKING ORTHOGONAL INTERACTION: SYNTHESIS OF SELECTIVE ANTIFOLATES AND CHARACTERIZATION OF DHFR INHIBITION

2.1 Introduction

Bioorthogonal ligand-protein interactions are a key element in chemical biology, allowing selective perturbation of a given protein's function within complex environments such as cell lysates, or even living cells. Small molecules ligands that exhibit high selectivity and affinity for a receptor protein can be leveraged to inhibit, activate or image the protein of interest (when the ligand is linked to a suitable fluorophore or other imaging agent). The antifolate trimethoprim (TMP), for example, has been used to selectively label *E. coli* DHFR (eDHFR) fusion proteins in living cells, allowing fluorescence microscopy analysis of eDHFR fusion proteins (32, 33). In addition, a heterodimeric conjugate of TMP with synthetic ligation factor (SLF) has been developed as a chemical inducer of dimerization (CID) and used to activate transcription in a yeast three-hybrid assay as well as modulate glycosylation in mammalian cells (49, 50). For most practical applications, the TMP-eDHFR interaction is bioorthogonal to mammalian systems. TMP interacts weakly with mammalian enzymes (K_i >1uM), however it strongly inhibits bacterial DHFR (K_i = 1 nM). While eDHFR is presumably, catalytically active within mammalian cells, it has nevertheless not been observed to interact with other known mammalian proteins.

DHFR have been the focus of intense drug discoveries efforts for several decades. The development of several antifolates that selectively inhibit DHFRs from different pathogenic organisms such as *Plasmodium falciparum* and *Pneumosytis carinii* has been a particular focus of these discovery efforts. These efforts have yielded several antifolates that exhibit nanomolar inhibitory activities towards *P. falciparum* DHFR (pfDHFR) and *P. carinii* DHFR (pcDHFR) while showing minimal activity against mammalian forms of the enzyme. Particular analogs are based on the substituted 5-benzyl pyrimidine scaffold, similar in structure to TMP. (39, 59-61)

Given the extensive knowledge available about selective antifolates, a key aim of the studies presented in this dissertation was the development of additional antifolate-DHFR pairs that could be used for live cell protein labeling and *in vitro* biochemical studies in addition to the established TMP-eDHFR pair. Of particular focus are Compound **1** and Compound **2** selective inhibitors for pfDHFR and pcDHFR, respectively. These compounds were shown to exhibit nanomolar potency against their respective targets while simultaneously exhibiting high selectivity over mammalian DHFR.

In this chapter, *in vitro,* enzyme inhibition studies were used to determine inhibition constants of substituted analogs of Compound **1** and Compound **2** against a soluble, truncated, TMP-resistant mutant of pfDHFR (K27E C59R S108N) and against pcDHFR, respectively. The results show that the substituted analogs retain the high potency and selectivity seen in the parent compounds.

2.2 Materials and Methods

2.2.1 Materials

QuickChange Multi Site- Directed Mutagenesis Kit was purchased from Stratagene (La Jolla, CA). Plasmid vectors containing DNA for *P. falciparum* DHFR soluble domain and *P. carinii* DHFR were kind gifts from Prof. Yongyuth Yuthavong and Prof. Victoria Cody, respectively. All chemicals were obtained from Sigma Aldrich, Inc. (Milwaukee, WI).

2.2.2 Synthesis

The following syntheses were originally developed and optimized by Dr. Rajasekhar Reddy. I subsequently performed each reaction detailed in this chapter. To synthesize the antifolates, a pyrimidine scaffold was obtained through an aldol condensation of an appropriately

substituted benzaldehyde with 3-morpholinopropanenitrile, followed by the replacement of the morpholine group with aniline and subsequent cyclization with guanidine.

2.2.2.1 Synthesis of **1a**, a 4'-substituted, triethyleneglycolamino derivative of Compound **1**

Scheme 1.

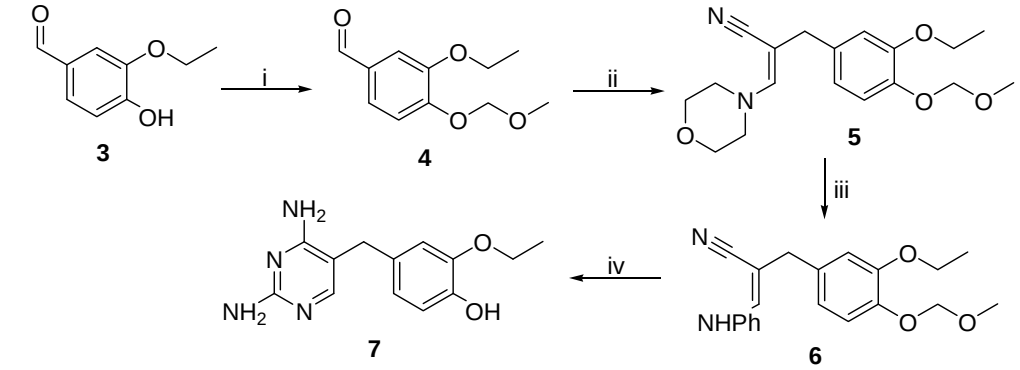

Reagents: i) MOM-Cl, DIPEA, DMAP, DCM; ii) 3-morpholinopropanenitrile (**22**), NaOMe, DMSO; iii) aniline hydrochloride, EtOH; iv) guanidine hydrochloride, NaOEt, EtOH.

Scheme 2.

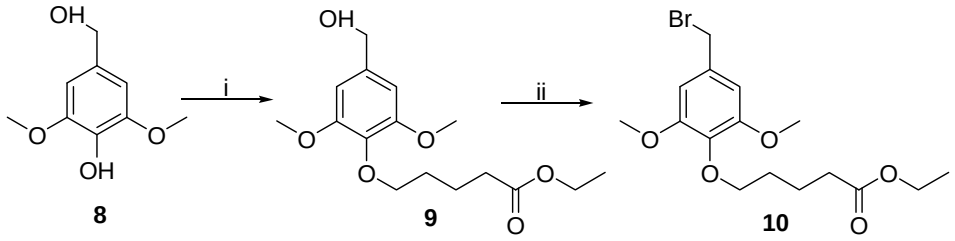

Reagents: i) ethyl-5-bromovalerate, DBU, DMSO; ii) PBr_3, DCM.

Scheme 3.

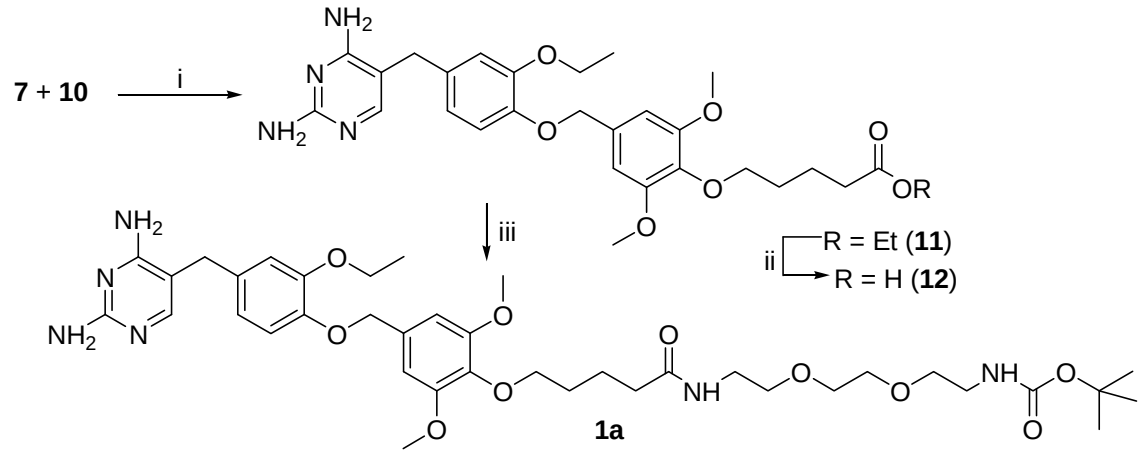

Reagents: i) DBU, DMSO; ii) 2N NaOH, EtOH; iii) *tert*-butyl-2-(2-(2-aminoethoxy)ethoxy)ethylcarbamate, EDCI, HOBt, DMF.

Synthesis of 1a: 3-Ethoxy-4-(methoxymethoxy)benzaldehyde (**4**): A mixture of 3-ethoxy-4-hydroxybenzaldehyde (**3**, 1 eq), DMAP (0.2 eq), and DIPEA (1.2 eq) in DCM (60 mL) was magnetically stirred and maintained at 0 ^{o}C under nitrogen atmosphere. MOM-Cl (1.2 eq) was added to the mixture dropwise. The reaction mixture was allowed to warm to room temperature, and it was stirred for 18 h, at which time cold HCl (140 mL of a 0.1N aqueous solution) was added. The organic and aqueous layers were separated by extraction with DCM (3x50 mL). The combined organic extracts were washed with water (60 mL) and brine (60 mL) and then dried over $MgSO_4$, filtered, and concentrated under reduced pressure. The resulting solid was subjected to flash chromatography (3:7 ethyl acetate/hexane elution) to obtain, 3-ethoxy-4-(methoxymethoxy) benzaldehyde (**4**, 4.02 g, 79%). ^{1}H NMR (400 MHz, $CDCl_3$) δ 1.46-1.60 (m, 3H), 3.52 (s, 3H), 4.15-4.18 (m, 2H), 5.31 (s, 2H), 7.25-7.27 (m, 1H), 7.39-7.42

(m, 2H), 9.85 (s, 1H); 13C NMR (125.7 MHz, $CDCl_3$) δ 14.6, 56.4, 64.4, 95, 110.8, 115.3, 126.1, 131.1, 149, 152.5; ESMS+ (*m/z*) 211 [*M*+H]+.

4-((2,4-Diaminopyrimidin-5-yl)methyl)-2-ethoxyphenol (7): *Step 1*. Sodium methoxide was freshly prepared by dissolving clean metallic Na (0.4eq) in anhydrous MeOH (10 mL). Methanol was evaporated under reduced pressure, and the solid was dissolved in DMSO (15 mL) to which 3-morpholinopropanenitrile (**22**) (1.2 eq) was added at 65 ^oC. The mixture was heated to 80 ^oC for 45 min, followed by the addition of 3-ethoxy-4-(methoxymethoxy)benzaldehyde (**4**), 3 g, 14.28 mmol) in 15 mL of DMSO over a 45 min period. After 2.5 h at 80 ^oC, the reaction mixture was cooled and extracted between EtOAc and H_2O acidified with citric acid. The organic fraction was washed with brine, dried over $MgSO_4$, filtered, and concentrated under reduced pressure. The product mixture was purified by flash chromatography (1:1 EtOAc/hexane elution) to afford 2-(3-ethoxy-4-(methoxymethoxy)benzyl)-3-morpholinoacrylonitrile (**5**) (1.2 g, 25%) as a yellow gum. ^1H NMR (400 MHz, $CDCl_3$) δ 1.41-1.45 (t, 3H, J = 4 Hz), 3.30 (s, 2H), 3.40-3.47 (m, 4H), 3.51 (s, 3H), 3.60-3.72 (m, 4H), 4.06-4.13 (q, 2H, J = 8, 16 Hz), 5.18 (s, 2H), 6.21 (s, 1H), 6.65-7.07 (m, 3H); ^{13}C NMR (100.6 MHz,$CDCl_3$) δ 14.8, 38.9, 49.4, 56.1, 64.4, 66.2, 75.4, 95.8, 113.7, 117.6, 120.4, 121.7, 134, 145.4, 148.8, 149.4 ppm.

Step 2. A mixture of compound **(5)** (1 eq) and aniline hydrochloride (1.2 eq) in anhydrous EtOH (15 mL) was refluxed for 1 h. In a separate flask, guanidine hydrochloride (5 eq) was added to a solution of NaOEt prepared by dissolving clean metallic Na (415 mg, 5 eq) in anhydrous EtOH (20 mL), and the flask was swirled manually for 10 min. The content of this flask was transferred to the mixture containing compound **(5)** and aniline hydrochloride. The mixture was refluxed for 20 h, then filtered while hot. Flash chromatography with 9:1

EtOAc/MeOH as the eluent to obtain product **(7)** (53%). ^{1}H NMR (500 MHz, CD3OD) δ 1.36-1.40 (t, 3H, *J* = 5.0 Hz), 3.59 (s, 2H), 3.90-4.10 (m, 2H), 6.60-6.65 (m, 1H), 6.70-6.80 (m,2H), 7.26 (s, 1H); ^{13}C NMR (125.7 MHz, CD3OD) δ 15.24, 32.64, 64.30, 106.86, 114.77, 115.83, 121.13, 131.10, 145.43, 146.88, 155.46, 162.39, 162.69; ESMS+ (*m/z*) 261 [*M*+H]+.

Ethyl 5-(4-(hydroxymethyl)-2,6-dimethoxyphenoxy)pentanoate (7): 4-(hydroxymethyl)-2,6-dimethoxyphenol **(8)** (1 eq) was dissolved in DMSO (4 mL) and DBU (1.2 eq) was added dropwise at room temperature. After 30 min, ethyl-5-bromovalerate (1.2 eq) was added slowly to the reaction mixture and stirred for 12 h. Water (~50 ml) was added and the product was extracted with EtOAc (3 x 50 mL). The combined EtOAc solution was washed with ~100 mL water, dried over MgSO4, filtered and the solvent was evaporated under reduced pressure. The crude product was subjected to flash chromatography (3:7 EtOAc/hexane) to obtain pure product **(9)** (83%). ^{1}H NMR (400 MHz, $CDCl_3$) δ1.22-1.26 (m, 3H), 1.79-1.83 (m, 5H), 2.36-2.37 (m, 2H), 3.83 (s, 6H), 3.93-3.96 (m, 2H), 4.10-4.20 (m, 2H), 4.61-4.62 (m, 2H), 6.57 (s, 2H); ^{13}C NMR (100.6 MHz,$CDCl_3$) δ 14.2, 21.4, 29.4, 33.9, 56, 60.1, 65.5, 72.6, 103.8, 136.4, 153.5, 174.

Ethyl-5-(4-(bromomethyl)-2,6-dimethoxyphenoxy)pentanoate (10): Ethyl-5-(4-(hydroxymethyl)-2,6-dimethoxyphenoxy)pentanoate **(9)** (1 eq) was dissolved in dry DCM (60 mL) and phosphorous tribromide (0.4 eq) was added to a solution at 0 °C. The mixture was allowed to warm up to room temperature and stirred for 1 h at which time was treated with cold water (30 mL). An extraction was performed with DCM (3 x 50 mL). The organic layer was washed with water (50 mL), a saturated sodium bicarbonate (50 mL) and brine (50 mL), dried over $MgSO_4$, filtered, concentrated in vacuo and purified by column chromatography (2:8 EtOAc/hexane) to obtain pure **(10)** (57%). ^{1}H NMR (500 MHz, $CDCl_3$) δ 1.23-1.26 (m, 3H),

1.78-1.90 (m, 5H), 2.35-2.42 (m, 2H), 3.84 (s, 6H), 3.92-3.98 (m, 2H), 4.10-4.20 (m, 2H), 4.45 (m, 2H), 6.60 (s, 2H); ^{13}C NMR (125.7 MHz, $CDCl_3$) δ 14.2, 21.4, 29.4, 33.9, 34.3, 56.1, 60.1, 72.7, 106.2, 132.9, 137.4, 153.4, 173.6; ESMS+ (*m/z*) 397 [*M*+Na]+.

Ethyl-5-(4-((4-((2,4-diaminopyrimidin-5-yl)methyl)-2-ethoxyphenoxy)methyl)-2,6-dimethoxyphenoxy)pentanoate (11): 4-((2,4-diaminopyrimidin- 5-yl)methyl)-2-ethoxyphenol **(7)** (1 eq) in DMSO (5 mL) was dissolved in DMSO and DBU (1.2 eq) was added dropwise at room temperature. After 30 min, ethyl 5-(4-(bromomethyl)-2,6-dimethoxyphenoxy)pentanoate (**10**) (1 eq) was added slowly to the reaction mixture and stirred for 12 h. The reaction mixture was extracted after adding water (~50 mL) with EtOAc (4 x 50 mL). The organic layer was washed with water, dried over $MgSO_4$, filtered and the solvent was evaporated under reduced pressure. The crude product was subjected to flash chromatography (9:1 EtOAc/MeOH) to obtain pure product **(11)** (40%). ^{1}H NMR (400 MHz, CD3OD) δ 1.22-1.26 (m, 3H), 1.36-1.40 (m, 3H), 1.68-1.90 (m, 4H), 2.30- 2.2.45 (m, 2H), 3.95-4.20 (m, 14H), 5.01 (s, 2H), 6.45-7.05 (m, 5H), 6.60 (s, 2H); 7.40 (s, 1H); ESMS+ (*m/z*) 555 [*M*+H]+.

5-(4-((4-((2,4-Diaminopyrimidin-5-yl)methyl)-2-ethoxyphenoxy)methyl)-2,6-dimethoxyphenoxy) pentanoic acid (12): Compound **11** (0.70 mmol) was dissolved in ethanol (10 mL) and 2N NaOH aqueous solution (1.5 mL) was added dropwise and the reaction mixture was stirred at room temperature for 10 h. Then the EtOH was removed under reduced pressure and the crude reaction mixture was adjusted to pH 4 with 1N HCl and extracted with EtOAc (6 x 50 mL). The combined organic extracts washed with brine and then dried over $MgSO_4$, filtered, and concentrated under reduced pressure (100 mg, 27%). The acid was used directly for the next step.

Synthesis of compound 1a: Compound **12** (1 eq) was dissolved in DMF (3ml) and EDCI (1.2 eq), HOBt (1.2 eq) and tert-Butyl-2-(2-(2-aminoethoxy)ethoxy)ethylcarbamate (1.2 eq) were added. The mixture was magnetically stirred for 24 h at room temperature. DMF was removed under vacuum and the residue was dissolved in ethyl acetate, extracted, washed with a saturated solution of sodium bicarbonate and with brine. The organic fraction was dried over $MgSO_4$; the solvent was removed under reduced pressure and purified by column chromatography (9:1 EtOAc/MeOH) to obtain pure product **(1a)** (35%). ^{1}H NMR (400 MHz, CD3OD) δ 1.30-1.41 (m,12H), 1.65-1.80 (m, 4H), 2.20-2.35 (m, 2H), 3.18-3.22 (m, 2H), 3.25-3.65 (m, 8H), 3.75 (s, 6H), 3.85 (s, 2H), 3.90-4.08 (m, 4H), 5.02 (s, 2H), 6.55-6.95 (m, 5H), 7.38 (1H); ^{13}C NMR (125.7 MHz, CD3OD) δ 13.9, 22.2, 27.3, 29, 32.2, 35.2, 38.8, 39.8, 55.2, 64.4, 69.2, 69.6, 69.8, 71.1, 72.5, 104.5, 107.6, 114.3, 115.3, 120.6, 131.7, 133.3, 147.1, 149.3, 150.2, 153.3, 157.5, 160, 163.4, 174.8; ESMS+ (*m/z*) 757 [*M*+H]+.

2.2.2.2 Synthesis of 2a, a 4'-substituted, triethyleneglycolamino derivative of Compound 2

Scheme 4.

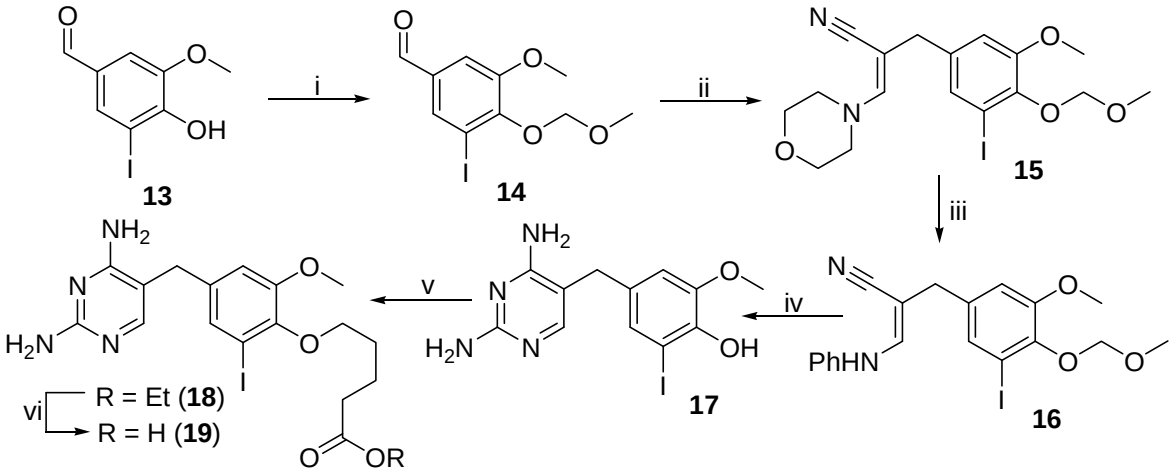

Reagents: i) MOM-Cl, DIPEA, DMAP, DCM; ii) **22**, NaOMe, DMSO; iii) aniline hydrochloride, EtOH; iv) guanidine hydrochloride, NaOEt, EtOH; v) ethyl-5-bromovalerate, DBU, DMSO; vi) 2N NaOH, EtOH.

Scheme 5.

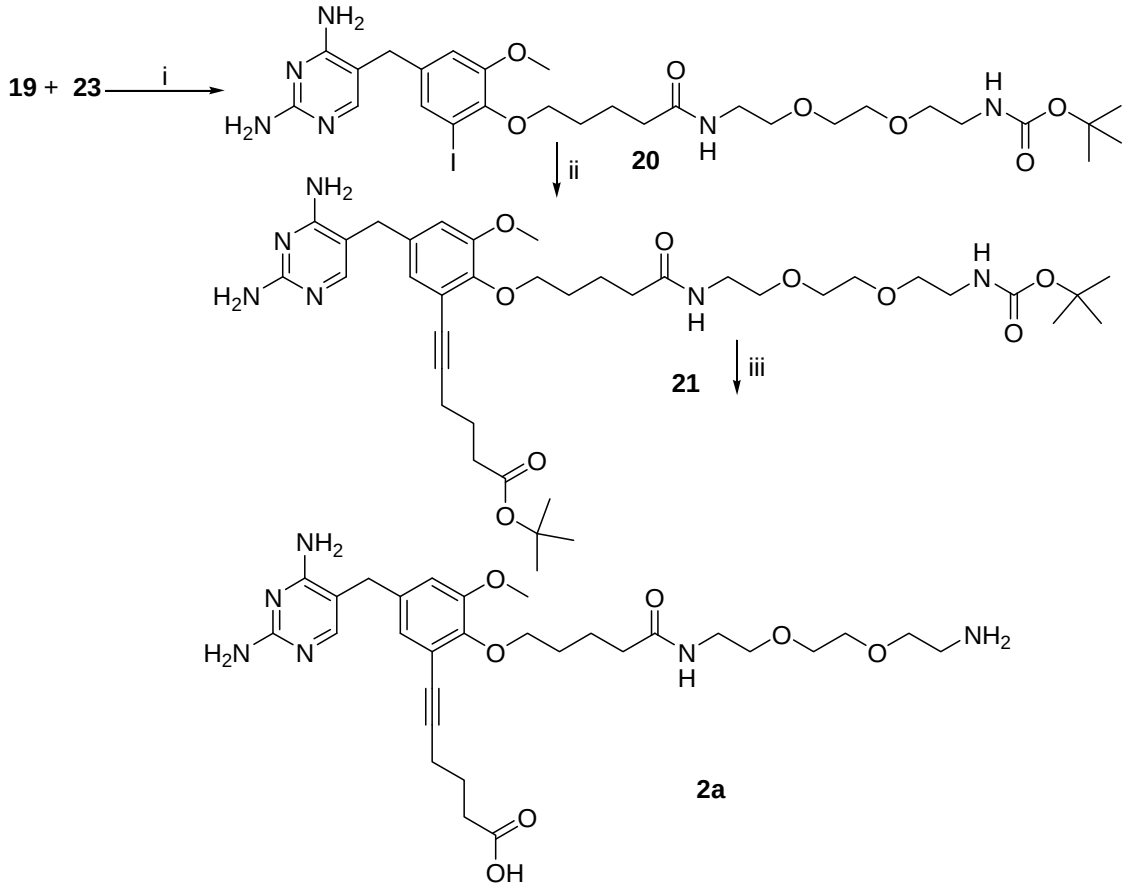

Reagents: i) **23**, EDCI, HOBt, DMF; ii) **24**, $(Ph_3P)_2PdCl_2$, $(Ph_3P)CuBr$, NEt_3, DMF; iii) TFA, DCM;

Scheme 6.

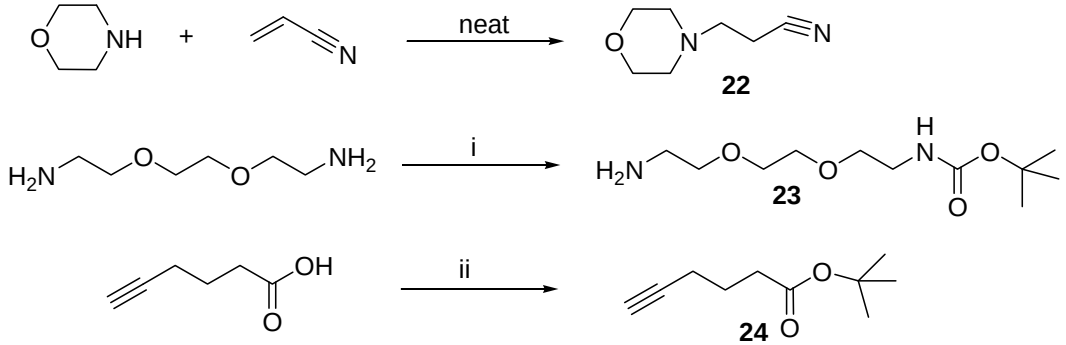

Reagents: i) di-*tert*-butyl dicarbonate, 10% TEA/MeOH; ii) trifluoroacetic anhydride, THF, *t*-butanol.

3-Iodo-5-methoxy-4-(methoxymethoxy)benzaldehyde (14): A solution containing 5-iodovanillin(**13**) (1 eq), DMAP (0.5 eq), and DIPEA (1.2 eq) in DCM (60 mL) was magnetically stirred and maintained at 0 ^{o}C (ice-water bath) under nitrogen atmosphere. MOM-Cl (1.2 eq), was added dropwise to the mixture. The resulting mixture was allowed to warm to room temperature and stirred for 18 h, at which time cold HCl (120 mL of a 0.1 N aqueous solution) was added. An extraction was performed with DCM (3x 50 mL) and combined organic extracts washed with water (60 mL) and brine (60 mL) and then dried over $MgSO_4$, filtered, and concentrated under reduced pressure. The resulting solid was subjected to flash chromatography (3:7 ethyl acetate/hexane elution) to obtain 3-iodo-5-methoxy-4-(methoxymethoxy) benzaldehyde (**14**) (81%). ^{1}H NMR (500 MHz, $CDCl_3$) δ 3.66 (s, 3H), 3.97 (s, 3H), 6.68 (S, 2H), 7.37 (s, 1H), 7.81 (s, 1H), 9.77 (s, 1H); ^{13}C NMR (125.7 MHz, $CDCl_3$) δ 56.5, 80.4, 98, 108.6, 131, 136, 146.4, 151.4, 189.4.

4-((2,4-Diaminopyrimidin-5-yl)methyl)-2-iodo-6-methoxyphenol (17): Step 1. Sodium methoxide was freshly prepared by dissolving clean metallic Na (0.6 eq) in anhydrous MeOH (10 mL). Methanol was evaporated under reduced pressure, and the solid was dissolved in DMSO (15 mL) to which 3-morpholinopropanenitrile (**22**) (1.2 eq) was added at 65^{o}C. The mixture was heated to 80 ^{o}C for 45 min, followed by the addition of 3-iodo-5-methoxy-4-(methoxymethoxy)- benzaldehyde (**14**) (1 eq) in 15 mL of DMSO over a 45 min period. After 2.5 h at 80 ^{o}C, the reaction mixture was cooled and extracted between EtOAc and H_2O acidified with citric acid. The organic fraction was washed with brine, dried over $MgSO_4$, filtered, and concentrated under reduced pressure. The product mixture was purified by flash chromatography (1:1 EtOAc/hexane elution) to obtain pure product 2-(3-iodo-5-methoxy-4-(methoxymethoxy)-benzyl)-3-morpholinoacrylonitrile (**15**) (22%) as a yellow gum. ^{1}H NMR (500 MHz, $CDCl_3$) δ

3.24 (s, 2H), 3.46-3.48 (m, 4H), 3.65 (s, 3H), 3.68-3.71 (m, 4H), 3.82 (s, 3H), 5.12 (s, 2H), 6.23 (s, 1H), 6.76 (s, 1H), 7.18 (s, 1H); ^{13}C NMR (125.7 MHz, $CDCl_3$) δ 38.5, 49.4, 56, 58.3, 66.2, 74.2, 92.6, 98.6, 113.1, 121.4, 130.2, 137.6, 145, 149, 152.1; ESMS+ (*m/z*) 445 [*M*+H]+, 462 [*M*+NH_3+H]+, 467 [*M*+Na]+.

Step 2. 2-(3-iodo-5-methoxy-4-(methoxymethoxy)benzyl)-3-orpholinoacrylonitrile (**15**) (1 eq) and aniline hydrochloride (1.5 eq) were dissolved in anhydrous EtOH (15 mL) and refluxed for 1 h. In a separate flask, guanidine hydrochloride (5 eq) was added to a solution of NaOEt prepared by dissolving clean Na (415 mg, 5 eq) in anhydrous EtOH (20 mL), and the flask was swirled manually for 10 min.The entire contents of the second flask (including the NaCl) were added to the first, and the combined mixture was refluxed for 20 h and then filtered while hot. Flash chromatography with 9:1 EtOAc/MeOH as the eluent to obtain the pure product (**17**) (53%). ^{1}H NMR (400 MsHz,$CDCl_3$) δ 3.58 (s, 2H), 3.82 (s, 3H), 6.80 (s, 1H), 7.10 (s, 1H), 7.28 (s,1H); 13C NM (125.7 MHz, $CDCl_3$) δ 32, 56.4, 84.8, 106.2, 113, 129.6, 133.6, 144.7, 147.3, 156.1, 162.5, 162.6; ESMS+ (*m/z*) 373 [*M*+H]+.

Ethyl-5-(4-((2,4-diaminopyrimidin-5-yl)methyl)-2-iodo-6-methoxyphenoxy)pentanoate (18): 4-((2,4-diaminopyrimidin-5-yl)methyl)-2-iodo-6-methoxyphenol **(17)** (1 eq) was dissolved in DMSO (5 mL) and DBU (1.2 eq) was added dropwise at room temperature. After 30 min, ethyl-5-bromovalerate (1.2 eq) was added slowly to the reaction and stirred for 12 h. Water (~50 mL) was added and the product was extracted with EtOAc (4 x 50 mL). The combined EtOAc solution was washed with ~100 mL water, dried over $MgSO_4$, filtered and the solvent was evaporated under reduced pressure. The crude product was subjected to flash chromatography (9:1 EtOAc/MeOH) to afford the pure product **(18)** (83%). ^{1}H NMR (500 MHz, $CDCl_3$) δ 1.23-1.26 (t, *J* = 5 Hz, 3H), 1.80-1.87 (m, 4H), 2.40-2.43 (t, *J* = 10

Hz, 4H), 3.61 (s, 2H), 3.79 (s, 3H), 3.91-3.93 (t, *J* = 5 Hz, 2H), 4.09-4.13 (q, *J* = 5, 10 Hz, 2H), 6.86 (s, 1H), 7.16 (s, 1H), 7.50 (s, 1H); ^{13}C NMR (125.7 MHz, $CDCl_3$) δ 13.1, 21.4, 29.1, 31.8, 33.5, 54.9, 59.9, 71.9, 91.7, 106.1, 113, 129.7, 137.1, 146.5,152.5, 154.3, 161.7, 163, 174; ESMS+ (*m/z*) 501 [*M*+H]+.

5-(4-((2,4-diaminopyrimidin-5-yl)methyl)-2-iodo-6-methoxyphenoxy)pentanoic acid (19): Ethyl-5-(4-((2,4-diaminopyrimidin-5-yl)methyl)-2-iodo-6-methoxyphenoxy)pentanoate (**18**) (1 mmol) was dissolved in EtOH (10 mL) and 2 N NaOH aqueous solution (2 mL) was added dropwise and the reaction mixture was stirred at room temperature for 10 h. Then the EtOH was removed under reduced pressure and the crude reaction mixture was adjusted to pH 4 with 1 N HCl and extracted with EtOAc (6 x 50 mL). The combined organic extracts washed with brine and then dried over $MgSO_4$, filtered, and concentrated under reduced pressure (300 mg, 64%). The acid was used directly for the next step.

Synthesis of compound 20: 5-(4-((2,4-diaminopyrimidin-5-yl)methyl)-2-iodo-6-methoxyphenoxy)pentanoic acid (**19**) (1 eq) was dissolved in DMF (6 mL) and EDCI (1.2 eq), HOBt (1.2 eq) and compound **23** (1 eq)were added. The mixture was stirred for 24 h at room temperature. The DMF was removed in vacuum, the residue was dissolved in ethyl acetate and washed with saturated sodium bicarbonate solution and then with brine solution. The organic phase was dried over $MgSO_4$, the solvent was removed under reduced pressure and purified by column chromatography (9:1EtOAc/MeOH) to obtain the pure compound (**20**, 300 mg, 56%). ^{13}C NMR (125.7 MHz, $CDCl_3$) δ 22.4, 27.4, 29.3, 31.6, 35.3, 38.9, 39.8, 55.1, 69.2, 69.6, 69.8, 72.2, 78.7, 92, 107.2, 113.2, 129.8, 136.1, 146.8, 148.2, 152.6, 163.6, 174.7; ESMS+ (*m/z*) 703[*M*+H]+, ESMS+ (*m/z*) 725 [*M*+Na]+.

Synthesis of compound 21: A stirred mixture of **20** (1 eq), alkyne (**24**) (1 eq), $(Ph_3P)_2PdCl_2$ (0.2 eq), $(Ph_3P)_3CuBr$ (0.01 eq), and NEt_3 (1 mL) in dry DMF (4 mL) was heated at 60 ^oC for 72 h. The solvent was removed in vacuum and extracted with ethyl acetate (4 x 50 mL). The combined organic phases were dried over $MgSO_4$, the solvent was removed under reduced pressure and purified by column chromatography (1:9 EtOAc/MeOH) to afford the pure compound (**21**) (38%). ESMS+ (*m/z*) 743 [*M*+H]+, ESMS+ (*m/z*) 765 [*M*+Na]+.

Synthesis of compound 2a: Trifluoroacetic acid (4 mL) was added to a solution of the *tert*-butyl ester **27** (0.03 mmol) in dichloromethane (1 mL) at 0 °C. The reaction mixture was stirred for 12 h at room temperature. After the reaction was complete, the solvent was removed under reduced pressure at room temperature and used directly for subsequent coupling reactions. ESMS+ (*m/z*) 587 [*M*+H]+, ESMS+ (*m/z*) 609 [*M*+Na]+.

Hex-5-ynoic acid tert-butyl ester (24): A dry flask was charged with hexynoic acid (1 g, 8.93 mmol) and purged with nitrogen. THF (40 mL) was added, and the solution was cooled to 0 °C. Trifluoroacetic anhydride (2.72 mL, 19.60 mmol) was added drop wise. The reaction was stirred at 0 °C for 2.5 h, then *t*-butanol (3 mL) was added slowly. After 1 h, the reaction was warmed to room temperature. The reaction was stirred for an additional 17 h, quenched with water (50 mL) and extracted with ether (4 x 50 mL). The combined organic layers were dried with $MgSO_4$, filtered and concentrated. The resulting oil was purified by flash chromatography (3% EtOAc in hexane) yielding **30** (1.2 g, 80 %) as a clear oil. ^1H NMR (400 MHz, $CDCl_3$) δ 1.44 (s,9H), 1.80 (pentet, *J* = 7.2 Hz, 2H), 1.96 (t, *J* = 2.7 Hz, 1H), 2.24 (dt, *J* = 2.7, 7.0 Hz,2H), 2.35 (t, *J* = 7.5 Hz, 2H); ^{13}C NMR (125.6 MHz, $CDCl_3$) δ 18.0, 24.0, 28.3, 34.4, 69.1, 80.5, 83.7, 172.7.

2.2.3 Plasmid preparation (pfDHFR mutagenesis)

Plasmid preparation (pfDHFR mutagenesis): Site directed mutagenesis (QuickChange™ Multi-sitedirected mutagenesis kit, manufacturer's instructions) was used to introduce mutations into plasmid pfDHFR(K27E)-GFP (C172T, T319A, C320A, G321T) to yield DNA encoding pfDHFR (K27E, C59R, S108N)-GFP. The mutations to the amino acids C59 and S108 were introduced in the plasmid by using the primers 5'-AGGTGGTAACCGCGCGGAAGTATTTCATGTCTAGAG-3' and 5'TTTTTTCGGAATCGATTCCCACTTGGTGCGGCCCATAACAACAAC-3'. To obtain the pfDHFR soluble domain from the fusion protein two stop codons were added to the plasmid sequence after the pfDHFR sequence. These codons were added by using the primer 5'-ATCTACAAGAAGACCAACTAGTAGGCTGGCTTCGCTGCTGGT-3' and the reverse compliment.

2.2.4 Protein expression and purification

MM Plates: 15g/L Agar, 1 x M9 salts (50 mM $Na_2HPO_4 \cdot 7H_2O$, 20 mM KH_2PO_4, 10 mM NaCl, 20 mM NH_4Cl), 0.4% glucose, 2 mM $MgSO_4$, 2 mM $CaCl_2$, 100 µg/mL ampicillin (AMP), 34 µg/mL chloramphenicol (CAM), 4 µM trimethoprim(TMP)).

Screening of active pfDHFR by bacterial complementation. *E. coli* strain BL21(DE3)pLysS was transformed (by electroporation, 1100V, time constant 5 usec.) with recombinant pfDHFR plasmids. Cells were harvested for 2 hr and plated onto minimal medium (MM) plates. Colonies obtained will contain active mutant pfDHFRs. Colonies are cultured for future protein expression.

pfDHFR expression. Single colonies of *E. coli* BL21(DE3)pLysS containing active mutant pfDHFRs were cultured in 60 mL of Luria-Bertani (LB) broth containing 100 µg/mL AMP, 34 µg/mL CAM for 3 hrs at 37 °C in orbital shaker at 250 r.p.m. Cells were added to 6 L

of LB broth containing 100 µg/mL AMP, 34 µg/mL CAM and incubated at 37°C in orbital shaker at 250 r.p.m until the OD_{595} was 0.6 at which time IPTG was added to a final concentration of 0.4 mM to induce protein expression. Cells were cultured for 24 hrs at room temperature in orbital shaker at 250 r.p.m. Culture was harvested by centrifugation at ~7000 *g* for 15min.

pfDHFR purification. Cells were resuspended in 25mL of Buffer A (20 mM potassium phosphate buffer, pH 7.0, 0.1 mM EDTA, 10 mM DTT, 20% glycerol) and lysed by Sonication for 10 min with a pulse cycle of 30 sec on, 30 sec off, on ice. Lysates were centrifuged for 1hr at 26,000 *g.* Cell lysate was circulated twice through a MTX-Agarose column (1.5 x 5cm), preequilibrated with Buffer A containing 0.2 M KCl. The column was washed with 50 mL of Buffer A supplemented with 1M KCl followed by the same buffer containing 50 mM KCl. In order to elute the proteins, thirty of Buffer B (50 mM TES, pH 7.8, 0.1mM EDTA, 10 mM DTT, 20% glycerol) containing ~ 4 mM H_2folate and 50 mM KCl were added to the column. The column was equilibrated after 1 column volume for 1 hr at which time the column was washed with the same buffer. Fractions (5mL) containing pfDHFR were combined and concentrated to 3 mL. H_2Folate was removed by size exclusion chromatography using a prepacked Sephadex G-25 column prequilibrated with buffer A.

2.2.5 Minimum Inhibitory Concentration (*E. coli* growth rate)

Luria-Bertani agar plates were prepared containing varying concentrations of inhibitors: Trimethoprim, Compound **1** and Compound **2**. *E. coli* strain DH5α was streaked onto the agar plates and plates were incubated at 37 °C for 24 hrs. The minimal inhibitory concentration (MIC) was reported as the lowest concentration at which no colonies formed.

2.2.6 Activity Assay

To determine the enzymatic activity of pfDHFR mutant proteins the change in optical density ar 340 nm (OD_{340}) was measured for 2.5 min. Two blank measurements were used to determine the activity of the enzymes. The first blank correspond to the change in OD_{340} of a solution containing Assay Buffer (50 mM TES pH 7.5, 75 mM 2-mercaptoethanol,1 mg/ml bovine serum albumin, BSA), 100 μM NADPH and 6 nM pfDHFR. The second blank corresponds to the change in OD_{340} of a solution containing 100 μM DHF and 6 nM pfDHFR in Assay Buffer. To measure the enzyme activity NADPH was added to the Assay Buffer to a final concentration of 100 μM in a quartz cuvette. The solution was mixed by inverting the cuvette several times, followed by addition of dihydrofolic acid (DHF) to a final concentration of 100 μM and mixing by inverting the cuvette. The reaction started upon addition of the enzyme to a final concentration of 6 nM. OD_{340} was measure using a Spectrophotometer kinetic program reading every 15 sec for 2.5 min. To calculate the activity of the enzyme the results were plotted as the OD_{340} as a function of time in min and the following equation was used to calculate the units per milligrams of protein.

$$\frac{Units}{mgP} = \frac{(\Delta OD_S - \Delta OD_{blank}) \times d}{12.3 \times V \times mgP / ml}$$

Where $\Delta OD_{/min\ blank}$ blank is the change in OD_{340} for the blank containing NADPH, $\Delta OD_{/min\ sample}$ is the change in OD_{340} for the reaction, 12.3 is the extinction coefficient for the DHFR reaction at 340 nM, *V* is the enzyme volume in milliliters, *d* is the dilution factor of the enzyme used, *mg P*/ml is the enzyme concentration of the original sample before dilution and *Units/mg P* is the specific activity in μmol/min/mg or protein where a unit will convert 1 μmole of DHF to tetrahydrofolic acid (THF) in 1 minute at pH 7.5.

2.2.7 Competitive Inhibition Assay

After determining the activity of the enzymes, inhibitory concentrations were determined using the same method described above in the presence of inhibitors. A plate reader was used to measure the change in OD_{340} upon addition of the enzyme preincubated with NADPH, to a solution of dihydrofolic acid and inhibitors. In a 96 Well plate, 100 µL of assay buffer were added to wells 2-12, into the first well 200 µl of inhibitor were added. The inhibitor was serially diluted in Assay Buffer in a 96 well plate, by transferring 100 µl from well 1 to well 2 and subsequently. NADPH and DHF were added to the inhibitor to a final concentration of 100 µM. Reaction started upon addition of the enzyme (~0.01 U, final concentration), preincubated with NADPH. Measurements were performed immediately. A binding isotherm was plotted using the program GraphPad Prism and fitting of the curve yield the IC_{50} values.

2.2.8 K_m determination

The method described above was used to determine the Michaelis-Menten biding constant, K_m. Using a Perkin Elmer Victor V and a 96 well plate, the change in absorbance at 340 nm was measured through time. DHF was serially diluted in Assay Buffer (50 mM TES pH 7.5, 75 mM 2-mercaptoethanol,1 mg/ml bovine serum albumin, BSA) starting at 100 µM maximum concentration. Upon addition of enzyme (~0.001U), preincubated with NADPH, the change in absorbance was measured through time. Results were plotted using GraphPad Prism as ΔOD_{340}/min against the concentration of DHF (µM).

2.3 Results and Discussion

2.3.1 Syntheses.

The general scheme for preparation of the antifolate analogs in this study first entailed aldol condensation of an appropriately substituted benzaldehyde with 3-morpholinopropanenitrile, followed by replacement of the morpholine leaving group with aniline

and subsequent cyclization with guanidine to yield 5-benzyl pyrimidine scaffolds (Scheme 1). Further substitutions yielded analogs **1a**, **2a**, which were analyzed for their inhibitory properties against pfDHFR and pcDHFR, respectively. Compounds **1a** and **2a** were coupled to amine-reactive fluorescein, as described in Chapter 3.

2.3.2 Minimum Inhibitory Concentration

An *E. coli* growth inhibition assay was performed to gauge the cross-reactivity of Compounds **1a** and **2a** against eDHFR. Thus, the minimal inhibitory concentration (MIC) was recorded as the concentration of inhibitor in which no *E. coli* colonies were observed to grow on minimal medium plates in the presence of inhibitors. Higher concentrations of Compounds **1a** and **2a** were required to inhibit *E. coli* growth than the nanomolar inhibitor, TMP. These results suggested that the putative pfDHFR and pcDHFR inhibitors were less efficacious against eDHFR, suggesting the possibility that they could be used simultaneously with TMP in live cell protein labeling experiments.

TABLE I
MINIMAL INHIBITORY CONCETRATION (μM values)

	TMP	**Compound 1a**	**Compound 2a**
E.coli	0.2	20	>100

2.3.3 IC_{50}

Expression and further purification of the pfDHFR (K27E C59R S108N), yielded an active enzyme as observed by a standard DHFR activity assay (Figure 11). In this assay,

absorbance at 340 nm is monitored over time as a proxy for substrate turnover, as it reflects reduction of the DHFR cofactor, NADPH. With this assay, a Michaelis binding constant for the substrate DHF (K_m) of 20 μM was observed, comparable to that reported previously for this enzyme Michaelis binding constant for the pfDHFR C59R S108N mutant (23 μM), reported by Sirawaraporn. (62)

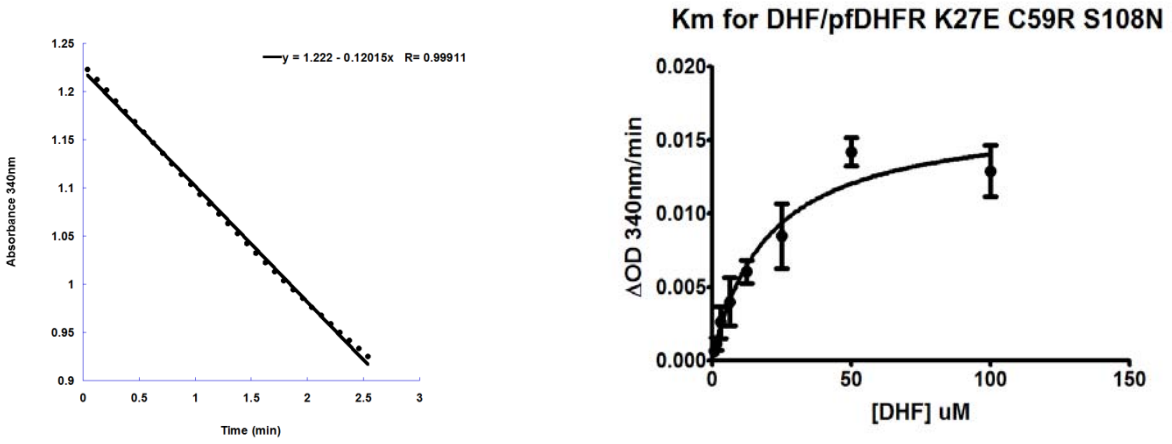

Figure 11: pfDHFR Characterization. Change in absorbance at 340 nm corresponding to the oxidation of NADPH through time to determine the enzyme activity. K_m determination by titrating different concentrations of DHF and measuring the change in absorbance at 340 nm corresponding to the oxidation of NADPH.

Inhibitory concentrations were determined in a similar fashion by titrating the enzyme and DHF against different concentrations of inhibitors. The observed inhibitory concentration for this Compound **1a** towards the mutant pfDHFR suggested submicromolar affinity (IC_{50} =

0.011μM). By using the Cheng Prushof equation (Equation 9), the inhibition constant for Compound **1a** was calculated in the presence of the substrate (K_i = 0.0018μM).

A complete picture of the relative inhibition activities of Compounds **1a**, **2a** and TMP against a panel of DHFR enzymes was obtained in collaboration with Prof. Sherry Queener at Indiana University. Using the same approach of measuring the rate of NADPH oxidation at 340 nm, the inhibitory concentration of Compound **1a** and Compound **2a** against rat liver DHFR, pcDHFR and *Toxoplasma gondii* DHFR (tgDHFR, a model enzyme used to assess potential pfDHFR inhhibitors) were measured. These results (Table II) indicated that Compound **1a** potently inhibited tgDHFR (IC_{50} = 0.032 μM) and pfDHFR (IC_{50} = 0.011 μM) while it poorly inhibited rat liver DHFR (IC_{50} = 6 μM). Compound **2a** also exhibited excellent potency and selectivity and strongly inhibited pcDHFR (IC_{50} = 0.025 μm) while it showed about 350-fold lower activity against mammalian DHFR. The inhibition data suggested that heterodimers of **1a** and **2a** linked to fluorophores at the amino functionality would retain effective potency against their putative targets, maintaining sufficient selectivity for bioorthogonal applications in mammalian systems.

TABLE II LIGAND BINDING CHARACTERIZATION (μM values)							
	DHF	**TMP**		**Compound 1a**		**Compound 2a**	
DHFR source	**K_m**	**IC_{50}**	**K_i**	**IC_{50}**	**K_i**	**IC_{50}**	**K_i**
E. coli	5.08	0.160	0.008	1.18	0.0562	ND	ND
Plasmodium falciparum(K27E C59R S108N)	19.84	>5000	---	0.011	0.0018	ND	ND
Rat liver	---	180	---	6	---	9.1	---
Pneumosistys carinii	---	12	---	1.373	---	0.025	---
Toxoplasma gondii	---	2.8	---	0.032	---	0.026	---

2.4 Conclusions

A complete characterization of the inhibitory activity of the antifolates **1a**, **2a**, and TMP against pfDHFR, pcDHFR, eDHFR and rat liver DHFR provides insights into the development of these compounds and proteins as potentially bioortogonal interacting pairs for applications in mammalian systems. As observed, both **1a** and **2a** exhibited high potency for their respective targets while retaining good selectivity over mammalian DHFR despite substitutions at the 4'-positions of the benzyl moiety. Moreover, **1a** also exhibited good selectivity for pfDHFR over eDHFR (30-fold, Table II). Thus, analogs of TMP and **2a** might be used to simultaneously target eDHFR and pfDHFR proteins in mammalian cells or cell lysates. One potential application is the simultaneously, multi-color imaging of two or more different DHFR fusion proteins upon labeling in live cells with appropriate ligand-fluorophore conjugates. Experiments to assess the feasibility of such an application are presented in the next chapter.

Chapter 3:

ASSESMENT OF PFDHFR AND PCDHFR INHIBITORS FOR SELECTIVE LABELING PROTEIN IN LIVE CELLS

3.1 Introduction

Genetically encoded fluorescent proteins make it possible to selectively impart fluorescence to proteins in living mammalian cells, enabling dynamic microscopic visualization of protein trafficking (14). However, the limited ability to modify fluorescent proteins' photophysical properties is a key limitation in developing more sophisticated, live cell microscopy techniques such as single molecule or superresolution imaging (15). Chemical protein labeling strategies make it possible to selectively tag target proteins with fluorophores or other functionalities directly in live cells. Here, what is required is a ligand that binds selectively and with high affinity (or covalently) to receptor protein or peptide sequence. With such a system, for example, more robust fluorophores can be synthetically coupled to the ligand and introduced into live cells that express the protein-receptor fusion.

In this chapter, the ability to selectively label fusions of pfDHFR or pcDHFR in living mammalian cells with fluorescent conjugates of **1a** or **2a**, respectively, was assessed. Compounds **1a** and **2a** were conjugated to acetylated 5(6)-carboxyfluorescein. It was anticipated that the acetylated fluorescein conjugates of these compounds would be cell permeable. Cultured NIH3T3 cells were transfected with genes encoding either pfDHFR or pcDHFR fused to a nuclear localization sequence. Cells were incubated with the fluorescent antifolates, washed and imaged using fluorescence microscope. The conjugate of **2a** appeared to be cell membrane impermeable, as no significant uptake of the compound into cells was observed. It was, however, possible to observe intracellular delivery of fluorescent **1a** and apparent labeling of nucleus-localized pfDHFR. However, overexpression of pfDHFR in mammalian cells seemed to result in high levels of cytotoxicity as determined by changes in cell morphology.

3.2 Materials and Methods

3.2.1 Materials

Dulbeccos modified eagle medium (DMEM), Dulbecco's phosphate buffered saline (PBS), fetal bovine serum, and Lipofectamine™ 2000 transfection reagent were purchased from Invitrogen (Carlsbad, CA). Cloning services were provided by Genscript, Inc. (Piscataway, NJ) NIH 3T3 cells were obtained as a gift from Prof. Wonhwa Cho. All chemicals were obtained from Sigma Aldrich, Inc. (Milwaukee, WI).

3.2.2 Plasmid construction

The genes for pfDHFR (K27E C59R S108N, 693bp) and pcDHFR (615bp) were inserted between the AgeI and XbaI restriction sites of the vector pLL1-NLS (Active Motif, Inc., Carlsbad, CA), yielding expression vectors that constitutively express pfDHFR (K27E, C59R, S108N) and pcDHFR as C-terminal fusions to three copies of the simian virus 40 large T-antigen nuclear localization sequence (DPKKKRKV).

3.2.3 Fluorescent labeling of pfDHFR fusion constructs

NIH3T3 fibroblast cells were cultured in Dulbecco's modified Eagle medium (DMEM) supplemented with fetal bovine serum (FBS; 10%), L-glutamine (2 mM), penicillin (100 IU μL-1), streptomycin (100 mg mL-1), HEPES (15 mM), and incubated in a humidified atmosphere at 37 °C and 5% CO2. Cells (ca. 80,000) were seeded into 6-well plates, and transient transfection was performed by using Lipofectamine2000™ reagent according to the manufacturer's protocol (2 μg DNA 6 μL Lipofectamine2000™). After ca. 6 h, the transfected cells were trypsinized and aliquoted (ca. 14,000 cells/well) into 8-well chambered coverslips (Nunc, Lab-Tek) and allowed to incubate another 12-18 h. For imaging, fluorescein conjugates (**1b**, or **2b**) were diluted (500

nM) in culture medium and incubated with the cells for ca. 15 min. at 37 °C. The cells were then washed 2X with PBS, and indicator-free DMEM without small molecule was added to the cells.

3.2.4 Microscopy

Epi-fluorescence microscopy of adherent live cells was performed using a Zeiss Axiovert 200 equipped with a 63X EC Plan Neofluar oil immersion objective (NA = 1.25). Excitation illumination was provided by a 100W Hg lamp. Excitation and emission light were selected by appropriate band-pass filters (Chroma Technologies, Inc. HQ480/40 (ex.), HQ535/50 (em.)). Images were detected using a Zeiss Axiocam MRM CCD camera, and captured with Zeiss Axiovision 4.6 software. Images were adjusted for brightness and contrast using NIH Image J and prepared for publication using Adobe Photoshop 5.5.

3.2.5 Synthesis of fluorescent conjugates.

Scheme 7.

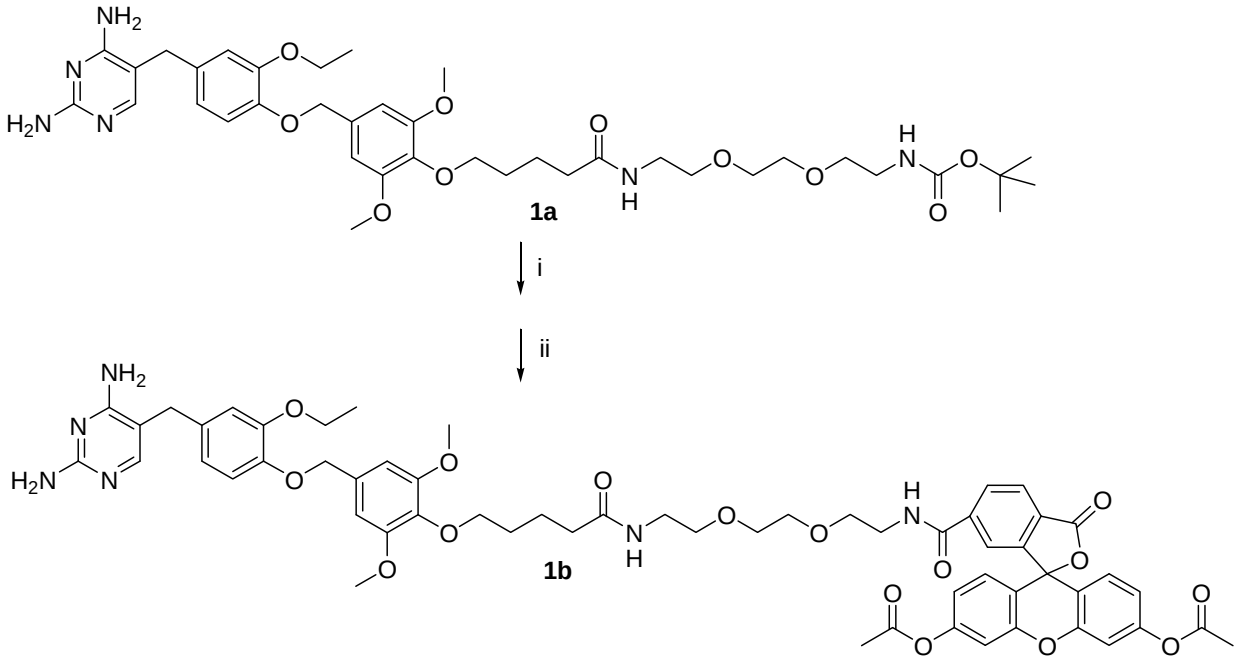

Reagents: i) TFA, DCM; ii) TEA, DMF, 5(6)-carboxyfluorescein diacetate N-succinimidyl ester.

Compound (**1b**). *Step 1.* Trifluoroacetic acid (0.1 mL) was added to a solution of compound **1a** (15 mg, 0.02 mmol) in dichloromethane (4 mL) at 0 ^{o}C. The reaction mixture was stirred for 12 h at room temperature. After the reaction was complete, the solvent was removed under reduced pressure at room temperature and the product used directly in the next step.

Step 2. To a well stirred suspension of deprotected **1a** (12 mg, 0.02 mmol) in DMF (2 mL), two drops of triethylamine was added. After 30 min, 5-carboxyfluorescein diacetate *N*-succinimidyl ester (12 mg, 0.02 mmol) was added and stirred the reaction mixture for 3 h at room temperature. The solvent was removed under reduced pressure and extracted with ethyl acetate (4 x 30 mL). The combined organic phases were dried over $MgSO_4$, filtered; the solvent was removed under

reduced pressure and purified by column chromatography (9:1 EtOAc/MeOH) to afford the compound (**1b**, 8 mg, 40%). ESMS+ (*m/z*) 1117 [*M*+H2O+H]+. *3*-

Scheme 8.

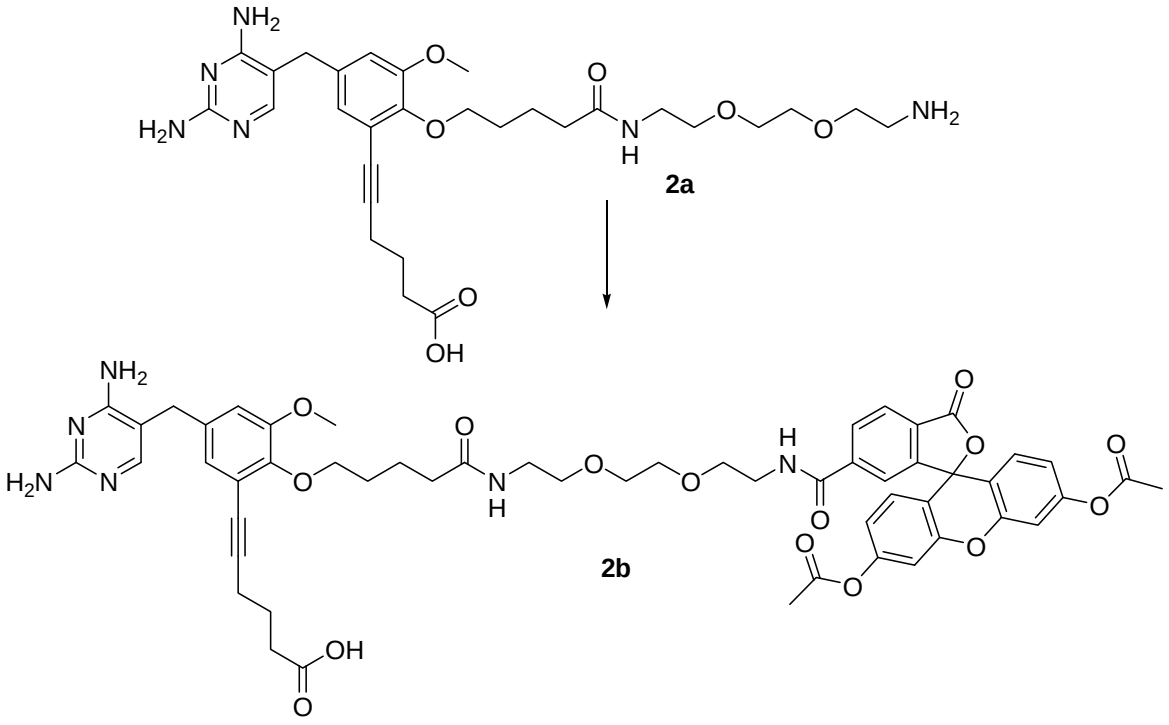

Reagents: TEA, DMF, 5(6)-carboxyfluorescein diacetate N-succinimidyl ester.

Compound (**2b**). To a well stirred solution of **2a** (20 mg, 0.03 mmol) in DMF (2 mL), three drops of triethylamine was added. After 30 min, 5-carboxy-fluorescein diacetate *N*-succinimidyl ester (20.05 mg, 0.04 mmol) was added and stirred the reaction mixture for 8 h at room temperature. The solvent was removed under reduced pressure and filtered, washed with diethyl ether, dichloromethane and cold ethyl acetate. The solid was collected and dried in vacuum, and purified by preparative TLC (1:9 MeOH/EtOAc). ESMS+ (*m/z*) 1029 [*M*+H]+, ESMS+ (*m/z*) 1047 [*M*+H3O]+.

3.3 Results and Discussion

The fluorescent analogs of **1a** and **2a** were prepared by reacting each analog with commercially available NHS esters of 5(6)-carboxy fluorescein diacetate. The choice of acetylated fluorescein was made in anticipation that the ester-protected fluorescein conjugates would readily permeate cell membranes, following which the esters would be removed by intracellular esterases, yielding the fluorescent dianion of fluorescein. This proved to be the case, as discussed below. However, the acetylated fluorescein proved to be highly unstable, undergoing apparent hydrolysis to the dianion in water. Moreover, this instability made it difficult to store stock solutions of the compound even in DMF at -20 °C. Attempts to prepare conjugates of **1a** to a more stable, isobutyryl protected fluorescein analog as reported by Miller *et al.* were unsuccessful (32).

Epifluorescence microscopy was used to determine the cell permeability and subcellular distribution of compound **1b** and its selective binding to pfDHFR K27E C59R S108N. An expression vector that targeted pfDHFR to the nucleus was prepared. Targeting was achieved by encoding pfDHFR soluble domain with an N-terminal fusion of three copies of the canonical simian virus 40 large T-antigen nuclear localization sequence (DPKKKRKV). NIH 3T3

fibroblast cells were transiently transfected with the vector. Approximately 24 h after transfection, the cells were incubated with low (500 nm) concentrations of **1b** and imaged microscopically.

Diffuse fluorescence was observed in all cells following incubation with **1b**, indicating effective cytoplasmic delivery and subsequent intracellular hydrolysis of the acetylated fluorescein moiety (Figure 12). In a subset of cells, distinct nuclear fluorescence with more brightly fluorescent nucleoli was observed, characteristic of the nucleus-targeting sequence. In cells that were pre-incubated with nonfluorescent **1a** prior to incubation with **1b**, no nucleus-specific fluorescence was observed. These microscopy results suggest that **1b** could enter cells and specifically label overexpressed pfDHFR (K27E C59R S108N).

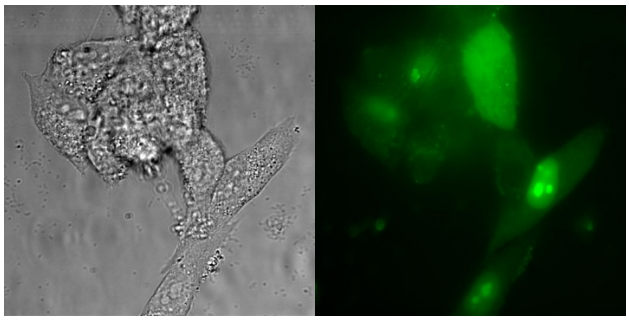

Figure 12. Selective chemical labeling of subcellularly targeted pfDHFR in living mammalian cells. Bright field (left) and fluorescence (right) micrographs show adherent NIH3T3 fibroblast cells transiently expressing nucleus- localized pfDHFR soluble domain (K27E, C59R, S108N). The cells were incubated in growth medium containing 500 nm **1b** for 15 min, washed two times with PBS, immersed in medium without compound and imaged.

Analogous imaging experiments were performed with **2b** and cells transfected with a vector encoding pcDHFR fused to the N-terminal nucleus localization sequence. However, we did not observe any intracellular fluorescence or nuclear staining. This result suggests that analogues of **2a** cannot passively diffuse into cells due to the presence of the anionic 5'-(5-carboxy-1-pentynyl) moiety.

3.4 Conclusions

Despite apparently successful labeling of nucleus-localized pfDHFR with **1b**, pfDHFR overexpression had a deleterious effect on cell morphology; cell rounding and/or blebbing was often seen (Figure 12). This effect, combined with the impermeability of **2b** and the difficulty of preparing stable fluorescent analogs of **1a** or **2a** led to a decision to abandon the live cell protein labeling aspects of this project. In the next two chapters, *in vitro* applications using bioorthogonal antifolate-DHFR pairs are presented.

Chapter 4:

SELECTIVE ANTIFOLATES AS TOOLS FOR IN-VITRO APLLICATIONS

4.1 Introduction

Over decades, extensive research has been devoted to find drugs to treat malaria. Finding effective drugs is difficult because of continuous mutations of the parasite *P. falciparum*. For example, mutations in the enzyme DHFR, make the parasite resistant to several antibiotics (37, 48). The search of new drugs is crucial to treat the disease. Advances in chemical biology and biotechnology can help to develop methods where inhibitors for this parasite can be identified from large chemical libraries. For example, a library of dihydrofolic acid analogs can be studied to identify antagonists with accuracy. Hence, it is needed a method with low signal to background ratio, and with low variability. TR-LRET can be used to develop such methods.

Antifolate conjugated to lanthanides complexes have been shown to be useful in TR-LRET to study biomolecular interactions (52, 56-58, 63). This is possible due to several advantages of these complexes: 1) efficient spectral separation of emission signals corresponding to large Stokes shifts (>150 nm) and multiple narrow emission bands; 2) minimal scattering and autofluorescence caused by long luminescence lifetimes (μs to ms); and 3) low probability of photobleaching permit prolonged detection.

In this chapter, TR-LRET is used to characterize the binding affinities of antifolates and DHFR-GFP fusion proteins. This characterization is extended to not only pure protein but also to cell lysates. This study indicates that this method can be employed in complex physiological environments. Also, an inhibition assay is developed using TR-LRET for *P. falciparum* DHFR. This method is suitable to detect inhibitors for pfDHFR. Given the large dynamic range in the signal, this assay can be translated to high throughput screening format (HTS).

4.2 Materials and Methods

4.2.1 Materials

Chemicals were purchased from Sigma-Aldrich. BugBuster, DNase, Halt protease inhibitor cocktail, PMSF, and imidazole were purchased from Thermo Fisher Scientific. High performance liquid chromatography (HPLC) was performed on a Beckman System Gold with a C18 column (GraceVydac, cat. no. 218TP54, 5 μm, 4.6 mm i.d. x 250 mm). Time-resolved luminescence intensity was measured using a 96-well plate reader (Perkin-Elmer, Victor 3 V) with 340 nm excitation (60 nm bandpass) and indicated emission filters (10 nm bandpass).

4.2.2 Synthesis

4.2.2.1 TMP-TTHA-cs124

The synthesis of TTHA dianhydride **(25)** and TMP-TTHA-cs124 was performed by Dr. Rajeshekar Reddy as previously reported (52).

4.2.2.2 C1a-TTHA-cs124 (27)

Step 1. Trifluoroacetic acid (TFA, 0.1 mL) was added to a solution of compound 1a (1.2 μmol) in dichloromethane at 0 ^{o}C. The reaction mixture was stirred for 12 h at room temperature. Then, the solvent was removed under reduced pressure at room temperature and the deprotected compound used directly in the next step.

Step 2. Compound **25** (ca. 12μmol) was dissolved in DMSO (1.2 mL) and TEA (20 equiv.) under nitrogen. Carbostyril 124 (**26**, 0.7 equiv.) was added and the solution stirred at room temperature for 10 min. Deprotected 1a dissolved in DMSO (0.8 mL) was added and the reaction stirred for 5 h. A few drops of water were added to quench the reaction, and the product **(27)** was purified directly from the reaction mixture by reverse-phase HPLC (20-min linear gradient, from 0% to 30% solvent B (solvent A, 0.1 M triethylammonium acetate (pH 6.5) plus

5% CH_3CN; solvent B, acetonitrile)). ESMS+ (m/z) 445 [M+H]+, 462 [M+NH_3+H]+, 467 [M+Na]+.

Scheme 9.

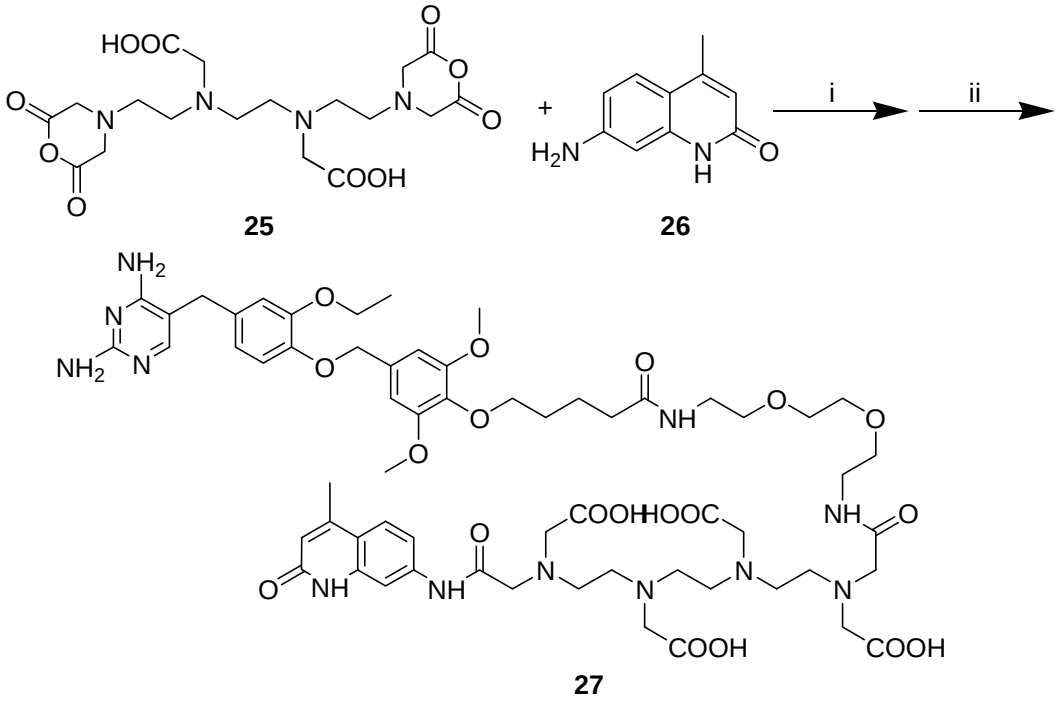

Reagents: i) TFA, DCM; ii) **1a**, DMSO, TEA

4.2.2.3 Methotrexate-TTHA-cs124 (35)

Compound **30**. Glutamic acid, N-[(9H-fluoren-9-ylmethoxy)carbonyl]-,1-(1,1-dimethylethyl) ester (**28**) (117 μmol), tert-butyl 2-(2-(2-aminoethoxy)ethoxy)ethylcarbamate (**23**) (1.2 eq), 1-Ethyl-3-(3-dimethyllaminopropyl)carbodiimide (EDCI, 1.2 eq), N-Hydroxybenzotriazole (HOBt, 1.2 eq) and triethylamine (TEA, 0.36mmol) in were dissolved in DCM (5.0 mL) was magnetically stirred for 18 hrs. The mixture was extracted (3x 50mL DCM) upon addition of saturated sodium bicarbonate wash. The organic layer was dried with $MgSO_4$, filtered and concentrated under reduced pressure. The resulting product was adsorbed into silica and subjected to flash chromatography, (1:4 Hexane/EtOAc), to obtain pure compound (**29**). ESMS+ (m/z) 656 [M+H]+, 678 [M+Na]+.

Compound **29** was subjected to Fmoc deprotection by dissolving in DMF containing 20% (w/v) pyridine. The mixture was stirred at room temperature for 20 min. and concentrated under reduced pressure to remove DMF and pyridine. The product (**30**) was used directly in the next step.

Compound **33**. 4-(N-((2,4-diaminopteridin-6-yl)methyl)-N-methylamino)benzoic acid (**31**) (30 μmol, 1 eq) and compound **30** (1.2 eq) in were dissolved in DMF (2.0 mL). HBtu (1.2 eq), HOBt (1.2 eq) and TEA (3 eq) were added while stirring, and the mixture was reacted for 16 h at room temperature. The reaction mixture was then washed with a saturated solution of sodium bicarbonate and with extracted ethyl acetate (3 x 25 mL). The organic layer was dried with $MgSO_4$ and concentrated under reduced pressure. The remaining substance was subjected to flash chromatography (1:10 MeOH/EtOAc) to afford pure compound (**32**). ^{1}HNMR (500MHz, CD3OD) δ 0.94-0.98 (t, 2H), δ1.31-1.41 (m, 2H), δ 1.55-1.64 (m, 2H), δ 1.64-1.70 (m, 1H), δ

1.45 (s, 9H), δ 1.5 (s, 9H), δ 9.0 (s, 2H), δ 2.15-2.25 (m, 5H), δ 2.25-2.4 (m. 4H), δ 6.86-6.88 (d, 2H), δ 7.74-7,76 (d, 2H) δ 8,5 (s, 1H) ESMS+ (m/z) 741 [M+H]+, 763 [M+Na]+.

Selective BOC deprotection was afforded by dissolving **32** in 4M HCL:dioxane and stirring for 30 min. on ice, and evaporating under reduced pressure to yield **33**.

MTX-TTHA-cs124 (35). Step 1. Compound **33** was washed two times with toluene and subjected to concentration under reduced pressure. The deprotected compound was dissolved in DMF.

Step 2. Compound **25** (ca. 12 μmol) was dissolved in DMF (1mL) and TEA (20 eq) under nitrogen. Carbostyril 124 (**26,** 0.7 eq) was added and the solution stirred at room temperature for 10 min. Compound **30** dissolved in DMF (0.8 mL) was added and the reaction stirred for 5 h. A few drops of water were added to quench the reaction, and the product (**34**) was purified directly from the reaction mixture by reverse-phase HPLC (20-min linear gradient, from 0% to 30% solvent B (solvent A, 0.1 M triethylammonium acetate (pH 6.5) plus 5% CH_3C N; solvent B, acetonitrile)).

Step 3. Fraction containing the purified product was concentrated, followed by a final deprotection with 30% TFA in DCM. Solvent was removed and compound **35** was confirmed by ESMS. ESMS+ (m/z) 1217 [M+H]+, 1240[M+Na]+.

Scheme 10.

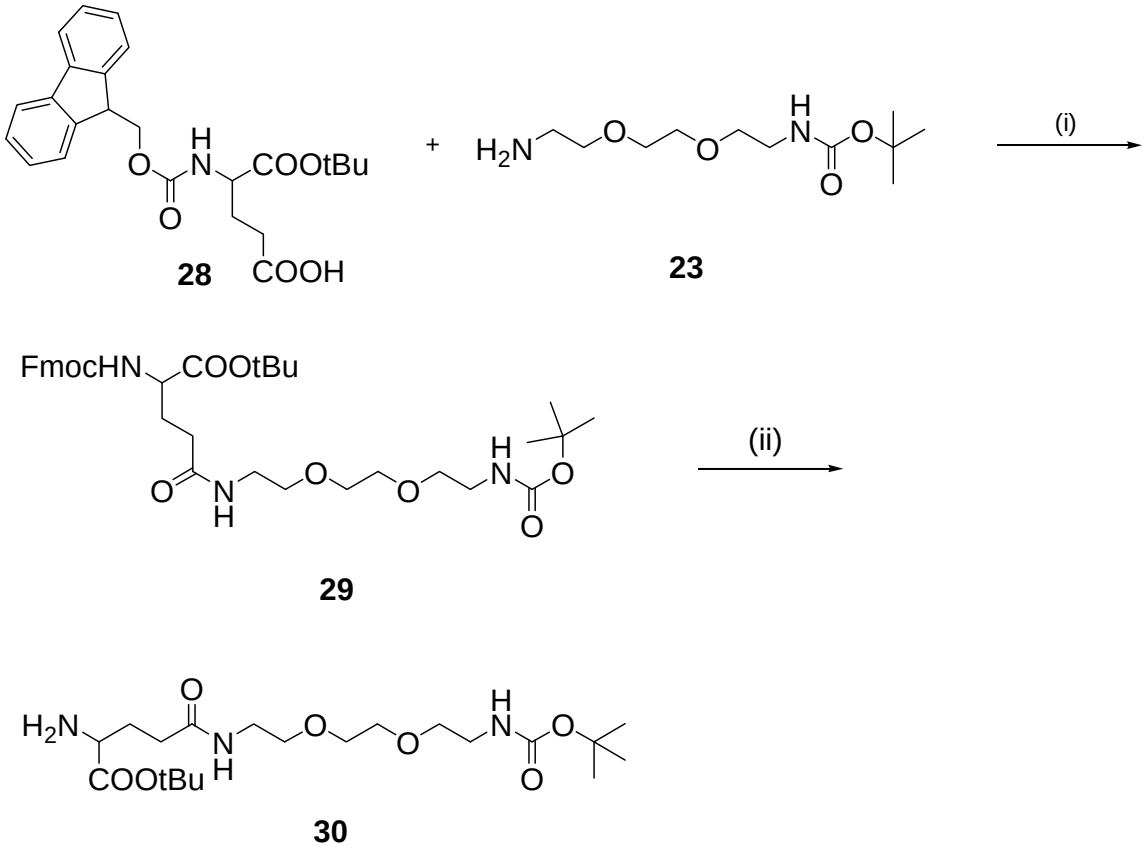

(i) EDCI, HOBt, TEA, DCM (ii) 20% pyridine, DMF

Scheme 11.

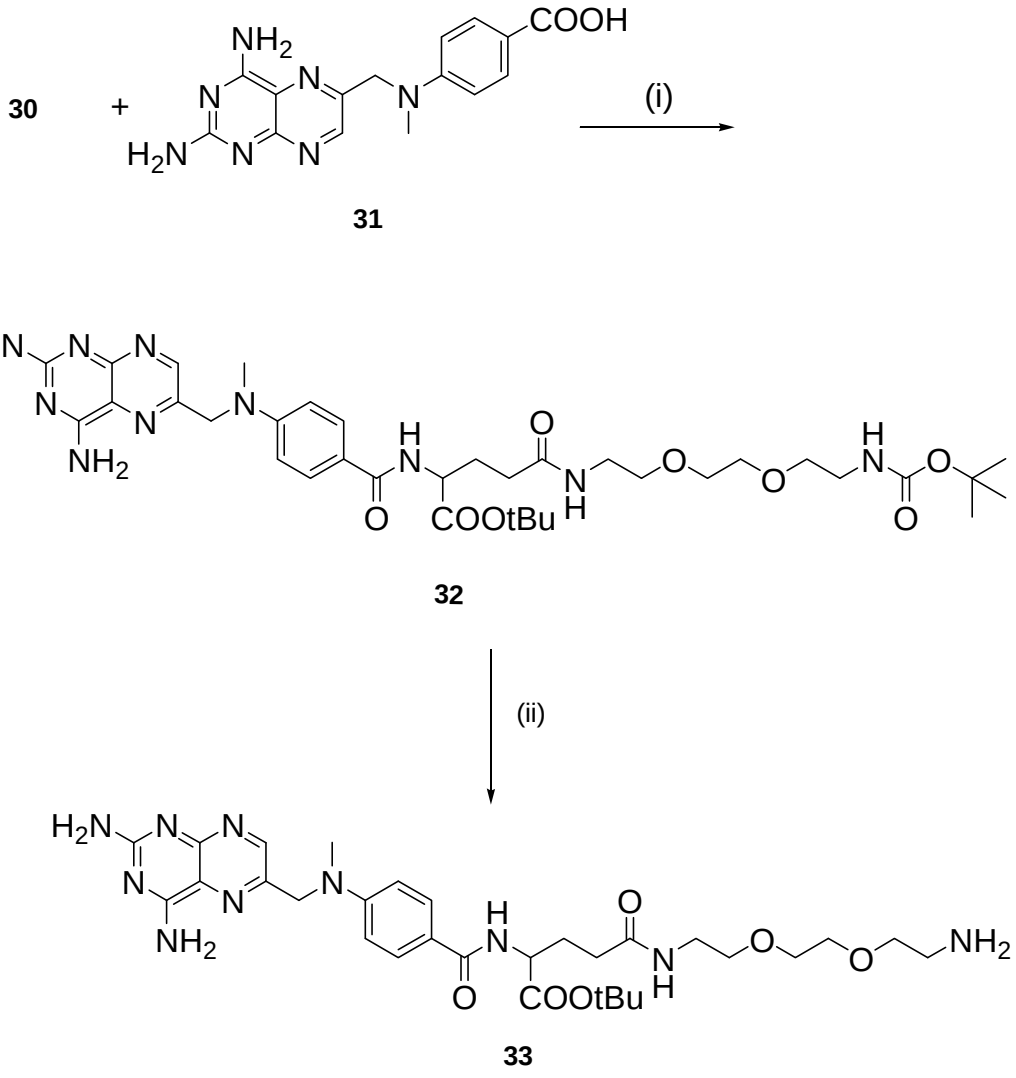

Reagents: (i) HBTU, HOBt, Et3N, DMF (ii) HCl:Dioxane

Scheme 12.

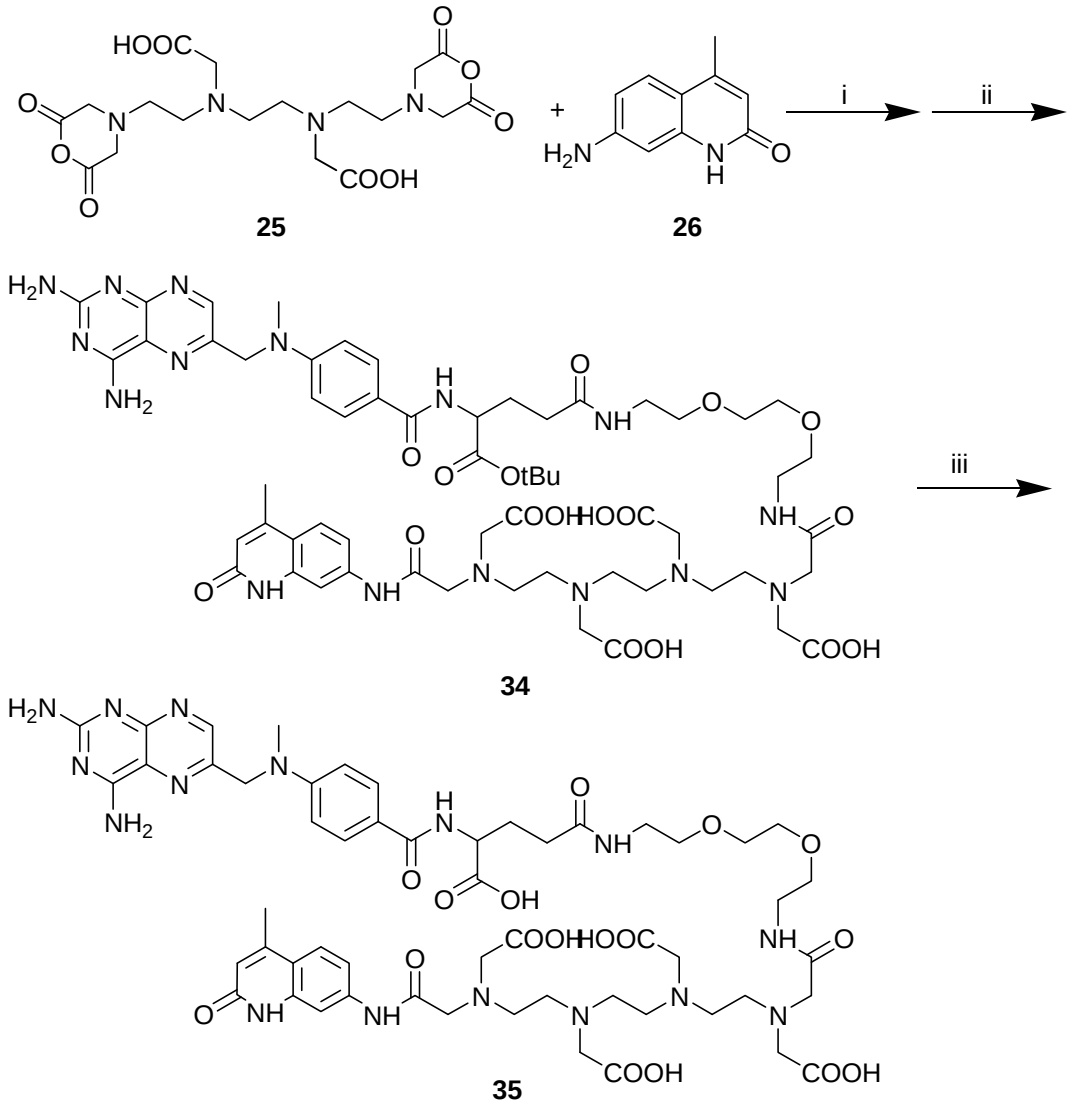

Reagents: (i) TEA, DMF (ii) EDCI, HOBt, DMF (ii) 30%THF,DCM

4.2.2.4 Addition of Metals

Compound concentration was obtained using measured absorptions and reported extinction coefficients for the fluorophores (cs124, ε = 10 500M 1 cm^{-1} at λ = 341 nm). Five equivalents of $TbCl_3$ 6H2O was added to the in TBS buffer (50 mM Tris 3HCl, 150 mM NaCl, pH 7.6) for TMP TTHA cs124 and water for MTX TTHA cs124 and C1a TTHA cs124 and allowed to stand for 30 min at room temperature before use.

4.2.3 Spectroscopic characterization of compounds.

The ability of the antifolate Tb^{3+} complexes to sensitize Tb^{3+} was characterized by obtaining the Tb^{3+} emission spectra of each complex, using a λ_{ex} = 340 nm.

4.2.4 Protein expression and purification

GFP-eDHFR was purified from the *E. coli* strain BL21 DE3 (pLysS) transformed with pRSETb-EGFP-eDHFR. A 5 mL Luria Bertani (LB) broth overnight culture was used to inoculate 500 mL of LB (Ampicillin, 100 mg/mL; chloramphenicol, 34 mg/mL). The 500 mL culture was grown at 37 °C, shaking at 200 rpm, to an OD_{600} of ~0.6, at which time expression of the protein was induced by the addition of IPTG to a final concentration of 1 mM. After growth for another 4 h, the cells were harvested by centrifugation. The pellet was lysed in 30 mL of lysis buffer (1X BugBuster Protein Extraction Reagent (Novagen), 10 μg/mL DNase, 1mM PMSF, 100 mM HEPES, 10 mM imidazole, pH 7.5). Samples were placed on an orbital shaker for 30 min, then centrifuged (15 000 rpm, 15 min, 4 °C) and applied to a column containing 2.0 mL of HisLink Protein Purification Resin (Promega). Following purification, the protein was concentrated (to ~10 μM), dialyzed with phosphate buffer (10mM K2HPO4, KH2PO4, pH7.4), and stored at 80 °C.

pfDHFR-GFP was expressed and purified was presented in Chapter 2.

4.2.5 Cell lysate preparation

Cell lysates containing GFP-eDHFR were obtained from 5.0 mL LB cultures of *E. coli* strain BL21 DE3 (pLysS) transformed with pRSETb-EGFP-eDHFR and treated to induce protein expression as described above. After growth and expression, the cells were harvested by centrifugation. The cell pellets were resuspended in 10 mM phosphate buffer (pH 7.4, with Halt Protease and Phosphatase Inhibitor, Thermo Scientific, Inc.) to a final concentration of 0.1 mg/μL. The cells were then lysed by sonicating for 1 min (2, 15 s on/off cycles) and recentrifuged (36,000 g, 15 min, 4 °C). The GFP-eDHFR concentration in the cell supernatant was determined by measuring the absorption of GFP at 484 nm (ε_{484} = 56 000 M^{-1} cm^{-1}).

4.2.6 Stability assay

In order to measure the stability of the TMP-lanthanide complex conjugate, an EDTA challenge assay was performed. The Tb^{3+} labeled antifolate was diluted to 50 nM in TBS, pH = 7.4, in a 1.5 mL centrifuge tube and EDTA was added to a final concentration of 10 mM (from a 0.02 M stock solution (H_2O/NaOH, pH = 8.0)), sample was vortexed for 1 min. TMP TTHA cs124 Tb^{3+} was aliquotted (100 μL) into 96-well plates, and the Tb^{3+} emission was measured over time using a time-resolved luminescence plate reader (time delay = 100 μs; measurement window =1400 μs; λ_{ex} = 340/60 nm; Tb^{3+}, λ_{em} = 545/10 nm). Lanthanide luminescence was normalized to the value measured at the first time point (10 min) and plotted vs time using Kaleidagraph (Synergy Software).

4.2.7 Binding affinity assay

The binding affinity of TMP-TTHA-cs124 complexed with Tb^{3+} for eDHFR was determined by measuring Tb^{3+}-to-GFP LRET in time-resolved mode. TMP conjugates (20 nM) were titrated in 96-well plates with either bacterial cell lysates containing GFP-eDHFR or

purified protein at concentrations ranging from ~0.5 nM to 1000 nM in assay buffer (50 mM K_2HPO_4, KH_2PO_4, 18 mM β-mercaptoethanol, 20 μM NADPH, pH 7.2). Titrations were done in triplicate for each sample. Time-resolved luminescence (time delay = 100 μs; measurement window = 1,400 μs, λ_{ex} = 340/60 nm) was measured at λ_{em} = 520/10 nm (LRET-sensitized GFP emission signal) and at λ_{em} = 615/10 nm (Tb^{3+} donor signal). For each well, the percent change in the donor-normalized LRET signal was calculated from the following equation:

$$\Delta LRETN\% = \frac{\left(\frac{520}{615}\right)_S - \left(\frac{520}{615}\right)_{-ctrl}}{\left(\frac{520}{615}\right)_{-ctrl}} \times 100 \qquad (11)$$

where $(520/615)_S$ represents the ratios of the emission signals at the indicated wavelengths for the sample well and $(520/615)_{-ctrl}$ represents the average emission ratio for three wells containing TMP-conjugate (20 nM) and no GFP-eDHFR. Using Kaleidagraph (Synergy Software), ΔLRETN% was plotted against protein concentration and dissociation constants were obtained by fitting the data to the following equation:

$$L = (L_{min} - (L_{min} - L_{max}) \times \frac{[L]_T + K_D + [P]_T - \sqrt{([L]_T + K_D + [P]_T)^2 - (4[L]_T[P]_T)}}{2[L]_T} \qquad (12)$$

where L_{min} is the ΔLRETN% of the TMP-Tb^{3+} complex with no receptor, L_{max} is the maximum ΔLRETN% signal observed at saturating receptor concentration, $[L]_T$ is the total amount of lanthanide complex used, and $[P]_T$ is the total amount of protein used. The binding affinity of

MTX-TTHA-cs124 complexed with Tb^{3+} for pfDHFR was determined by measuring Tb^{3+}-to-GFP LRET in time-resolved mode. MTX conjugate (20 nM), was titrated in 96-well plates with purified protein at concentrations ranging from ~0.5 nM to 1000 nM in assay buffer (50 mM TES pH 7.5, 75mM 2-mercaptoethanol, 1 mg/ml bovine serum albumin, BSA). Analysis was performed as above.

4.2.8 Competitive Inhibition Assay

The inhibition constant for MTX and Compound **1** was measured using TR-LRET. The energy transfer between pfDHFR K27E –GFP and MTX-TTHA-cs124 (Tb^{3+}) was measured in the presence of unlabed antifolate (MTX and compound **1a**). The concentrations of MTX-TTHA-cs124(Tb^{3+}) and pfDHFR K27E-GFP were selected such that 90% of the MTX-Tb^{3+} was bound, avoiding enzyme depletion and overestimation of K_i. A complex of pfDHFR K27E-GFP (30 nM), NADPH (10 μM) and MTX-TTHA-cs124(Tb^{3+}) (3 nM) was titrated into 96-well plate containing unlabeled MTX (concentration ranging from 0.122 nM to 250 nM) and also the complex was titrated into a 96-well plate containing unlabeled compound **1a** (concentration ranging from 0.244 nM to 500 nM) in assay buffer containing 50 mM TES pH 7.5, 75 mM 2-mercaptoethanol,1mg/ml BSA. Time-resolved luminescence (time delay = 100 μs; measurement window = 1400 μs, λ_{ex} = 340/60 nm) was measured at λ_{em} = 520/10 nm (LRET-sensitized GFP emission signal) and at λ_{em} = 615/10 nm (Tb^{3+} donor signal). The data was analyzed using the program GraphPad Prism, by plotting the log of the concentration of unlabeled ligand against the TR-LRET signal. The curve was analyzed with the following equation:

$$\Delta LRET = L_{\min} + \left(L_{\max} - L_{\min}\right)/\left(1 + 10^{([I] - \log EC50)}\right) \tag{13}$$

$$\log EC50 = \log\left(10^{\log Ki \times (1 + [S]/K_{Ds})}\right) \tag{13a}$$

where L_{min} and L_{max} represent the minimum and maximum TR-LRET signals, [I] represents the concentration (nM) of unlabled antifolate, [S] is the concentration (nM) of MTX-TTHA-cs124(Tb^{3+}) complex used and K_D is the dissociation constant of the MTX-TTHA-cs124(Tb^{3+}) complex for pfDHFR K27E pfDHFR-GFP. K_i is the fitted parameter; the inhibition constant for the unlabeled antifolate.

4.3 Results and Discussion

4.3.1 Synthesis and characterization of luminescent antifolate-terbium complex conjugates.

Synthesis of C1a-TTHA-cs124 (33) and MTX-TTHA-cs124 (42) was achieved by reacting the dianhydride of TTHA with approximately equimoloar amounts of the amino derivatives of each antifolate and cs124 (Schemes 7, 10). Each complex was purified using reverse-phase HPLC and identified by electrospray mass spectrometry. A triethylene glycol-amino derivative of MTX was prepared by first reacting an orthogonally protected glutamic acid derivative with a mono-BOC-protected triethylene glycol diamine (29). Subsequent conjugation of the product (36) to 4-(N-((2,4-diaminopteridin-6-yl)methyl)-N-methylamino)benzoic acid yielded a MTX analog that was selectively functionalized at the γ-carboxylate position (39). This strategy made it possible to conjugate MTX without disrupting its affinity for DHFR.
The antifolate conjugates were metallated with excess Tb^{3+}, and the fluorescence emission spectra for each complex were acquired (Figure 13).

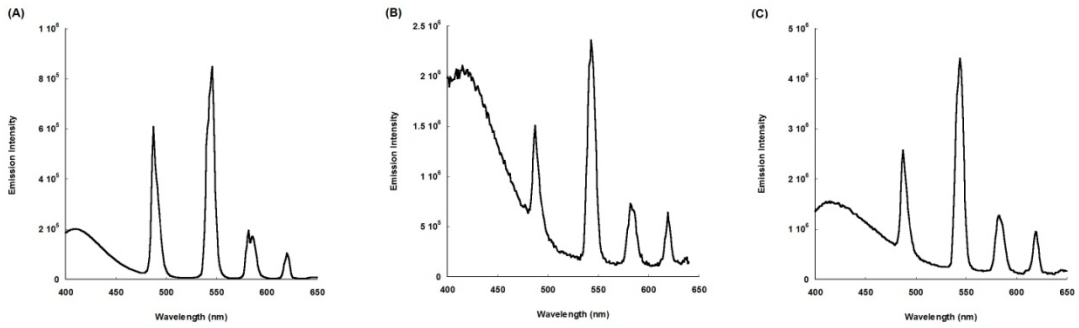

Figure13: Emission spectra (λ_{ex} = 340 nm) of Tb^{3+} complexes of (A) TMP-TTHA-cs124 (B) C1a-TTHA-cs124 (C) MTX-TTHA-cs124 .

As observed in the emission spectra, all compounds exhibit characteristic Tb^{3+} emission spectra. However, C1a-TTHA-cs124(Tb^{3+}) shows a broad, intense emission band at 425 nm. This band corresponds to the fluorescence emission of cs124. The presence of this band indicates that sensitization of Tb^{3+} does not occur efficiently. Hence, C1a-TTHA-cs124(Tb^{3+}) cannot be used as an effective LRET donor. On the other hand, both the TMP and MTX Tb^{3+} complexes showed more efficient sensitized Tb^{3+} emission .

4.3.2 Stability of TMP-TTHA-cs124

Given the photophysical properties of the lanthanides complexes, different applications can be exploited where complex samples are used, improving signal to background ratios, for example, in living cells or cells extracts. Under these conditions, it is important that the complexes remain stably metallated in the presence of other chelators or metal ions which may be present. For this reason, the relative stability of the Tb^{3+} complexes of TMP-TTHA-cs124 and the commercially available DTPA-cs124 was analyzed.

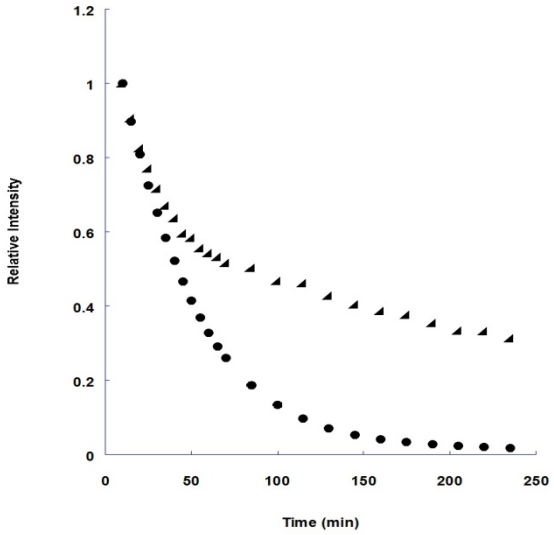

Figure14: Relative emission intensity over time in the presence of EDTA for TMP-TTHA-cs124 and DTPA-cs124 Tb^{3+} complexes

To compare relative stability, the Tb^{3+} emission intensity over a period of 3 h in the presence of EDTA for the Tb^{3+} complexes of the TMP-TTHA cs124 and of DTPA-cs124 (Figure 14). In the presence of 10 mM of EDTA, the Tb^{3+} emission intensity for each compound rapidly decreases initially and then stabilizes after ~75 min. After ~3 h, the TMP-TTHA-cs124(Tb^{3+}) retained ~55% of its initial intensity, while the luminescence of DTPA-cs124(Tb^{3+}) was reduced much more (~9% initial intensity). These results suggest that TMP-TTHA-cs124 and analogous antifolate Tb^{3+} complexes may provide analytically useful signals for extended time periods in cell lysates or other complex matrices where competitive chelators are present.

4.3.3 Affinity of TMP-TTHA-cs124 for purified GFP-eDHFR and GFP-eDHFR expressed in cell lysates

A potential benefit of stable antifolate-Tb^{3+} complexes is to label proteins within live cells or cell extracts, which can be applied when highly purified protein cannot be obtained. Therefore, I quantitatively analyzed the binding of TMP-TTHA-cs124(Tb^{3+}) to GFP-eDHFR, both in a purified buffer solution and in a bacterial lysate that was made to overexpress the protein.

The dissociation constants for the binding of TTHA-cs124(Tb^{3+}) to eDHFR was determined by measuring Tb^{3+}-sensitized GFP emission in time-resolved mode. The assay was performed in two layouts: 1) purified GFP-eDHFR was titrated against a fixed concentration (20 nM) of TMP-TTHA-cs124(Tb^{3+}) in assay buffer (50 mM K2HPO4, KH2PO4, 18 mM β-mercaptoethanol, 20 μM NADPH, pH 7.2); and 2) a lysate of *E. coli* expressing GFP-eDHFR was diluted directly into assay buffer without purification and titrated against 20 nM of TMP-TTHA-cs124(Tb^{3+}).

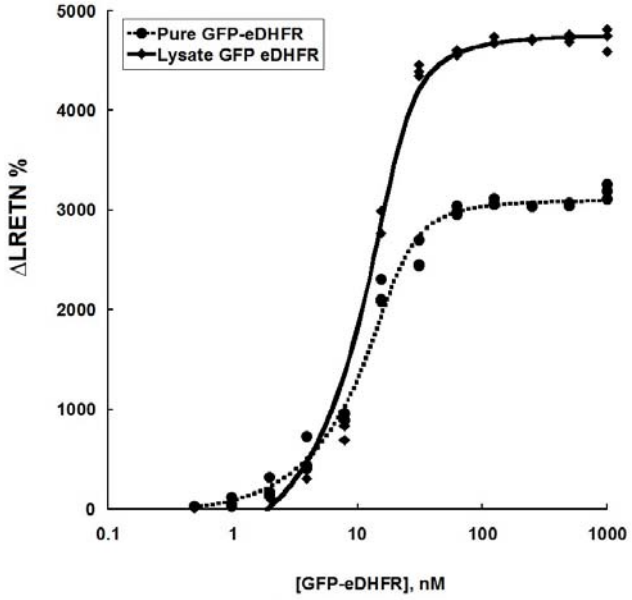

Figure15. Intramolecular, luminescence resonance energy transfer (LRET) between eDHFR-bound Tb^{3+} complex of TMP-TTHA-cs124 and GFP. Increasing concentrations of either purified eDHFR-GFP or a bacterial lysate containing the protein were titrated against a constant concentration (20 nM) of compound. Sensitized GFP emission (520 nm) and Tb^{3+} emission (615 nm) was detected after a time delay of 100 μs, upon pulsed excitation with near-UV light (340 nm). The y-axis represents the percent change in the 520/615 emission ratio. Lines represent nonlinear least-squares fit to the data

Using a time-resolved luminescence plate reader, the sensitized, long-lifetime (>100 μs) GFP emission at 520 nm (the LRET signal) and the Tb^{3+} donor emission signal (615 nm) were measured. The percent change in the 520 nm/615 nm emission ratio was plotted versus GFP-eDHFR concentration, revealing characteristic binding isotherms (Figure15). Nonlinear, least-squares fits of the data showed that the dissociation constants for binding to GFP-eDHFR equaled ~1.5 nM for TMP-TTHA-cs124 compounds under each assay condition. The ability to quantitatively measure binding events in a complex mixture, coupled with the large dynamic range of the LRET signal, suggests that antifolate lanthanide complex conjugates could be used for high-throughput screening or quantification of biomolecular interactions, especially in cases where highly pure biochemical preparations cannot be obtained.

4.3.4 Affinity of MTX-TTHA-cs124 for pfDHFR-GFP

The binding affinity of the antifolate MTX against purified pfDHFR K27E was assessed by using the same TR-LRET approach. A GFP – pfDHFR K27E fusion protein was used for this assay. Because C1a-TTHA-cs124 is not a good Tb^{3+} sensitizer, the pfDHFR fusion protein was titrated against a fixed concentration of MTX-TTHA-cs124(Tb^{3+}) (20 nM) in assay buffer (50mM TES pH 7.5, 75mM 2-mercaptoethanol,1mg/ml, BSA). A binding isotherm was obtained and the dissociation constant was equal to 4.0 ± 0.5 nM.

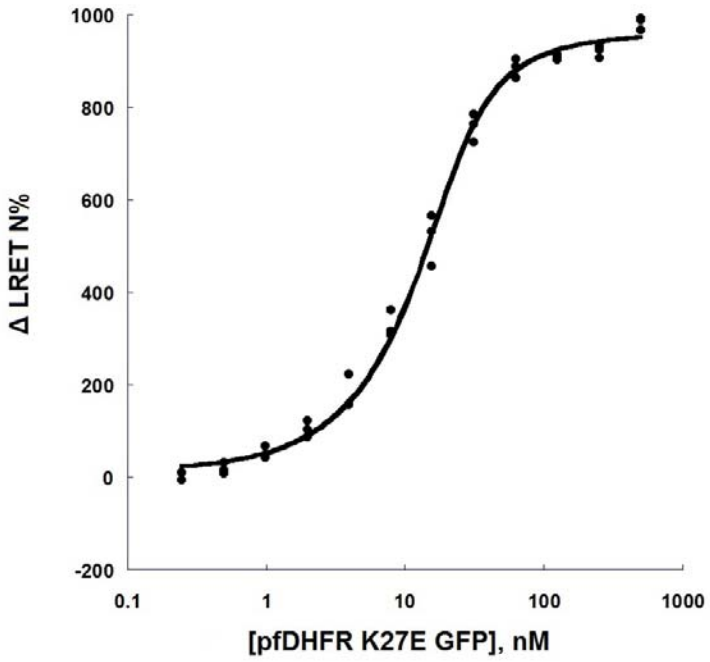

Figure 16. Intramolecular, luminescence resonance energy transfer (LRET) between pfDHFR-bound MTX-TTHA-cs124(Tb^{3+}) and GFP. Increasing concentrations of purified pfDHFR(K27E)-GFP was titrated against a constant concentration (20 nM) of MTX-TTHA-cs124(Tb^{3+}). Sensitized GFP emission (520 nm) and Tb^{3+} emission (615 nm) was detected after a time delay of 100 μs, upon pulsed excitation with near-UV light (340 nm). The y-axis represents the percent change in the 520/615 emission ratio. Lines represent nonlinear least-squares fit to the data.

4.3.5 Competitive inhibition

A competitive inhibition for pfDHFR was developed using TR-LRET. The assay for pfDHFR was designed using MTX-TTHA-cs124(Tb^{3+}) as a labeled ligand, competing with an unlabled antifolate. The soluble truncated DHFR domain from the thymidylate synthase complex of P. *falciparum* (pfDHFR(K27E)-GFP, c.a. 30 nM), was preincubated with 10 μM NADPH and 3 nM MTX- TTHA-cs124(Tb^{3+}). Unlabeled antifolate was then titrated against the pre-formed, labeled conjugate-protein complex (pfDHFR-MTX Tb^{3+}) was titrated against an unlabled antifolate. To validate the method, the first antifolate analyzed was unlabeled MTX. Upon titration of the unlabeled MTX an inhibition binding isotherm was observed and the inhibition constant obtained by non-linearly fitting the data to equation 13. From this results it was observed that after 1hr of incubation, equilibrium was reached and the obtained K_i value for unlabeled MTX was comparable to the K_D value for MTX-TTHA-cs124 Tb^{3+} ($K_i = 5.6 \pm 0.4$ nM vs $K_D = 4.0 \pm 0.5$ nM).

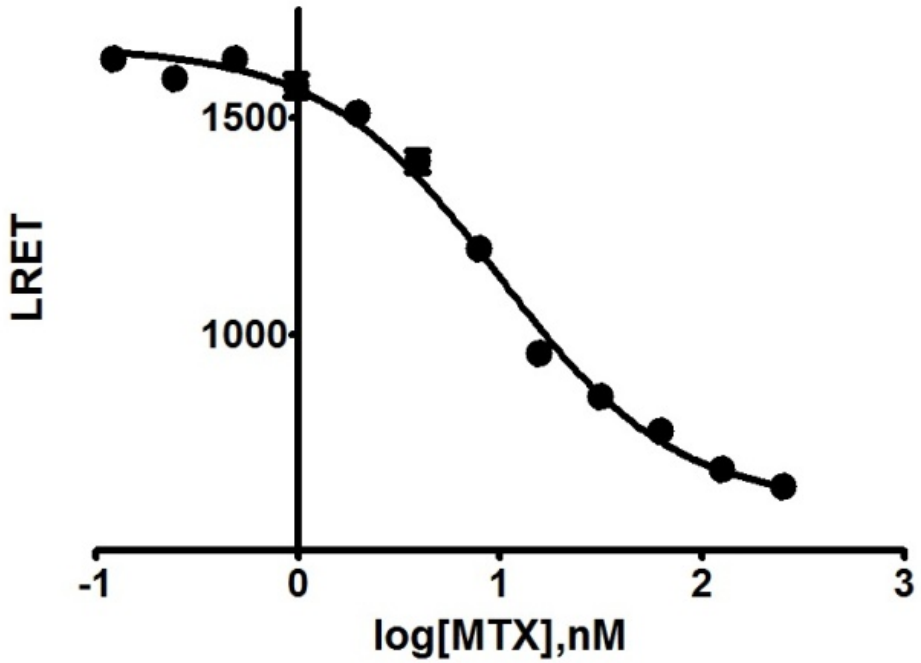

Figure 17: Intramolecular, luminescence resonance energy transfer (LRET) between pfDHFR-bound Tb^{3+} complex of MTX-TTHA-cs124 and GFP. Increasing concentrations of unlabeled MTX were titrated against a constant concentration (3 nM) of MTX-TTHA cs124(Tb^{3+}) and 30 nM of pfDHFR K27E-GFP. Sensitized GFP emission (520 nm) and Tb^{3+} emission (615 nm) was detected after a time delay of 100 μs, upon pulsed excitation with near-UV light (340 nm). The y-axis represents the GFP sensitized emission. Line represents nonlinear least-squares fit to the data.

An analogous experiment was performed using Compound **1a** as the competitive inhibitor. In this case, equilibrium was reached after 1 h, and an inhibition binding isotherm was obtained. A non-linear fit to equation 13 yielded a K_i of 38 $\pm$ 8 nM was observed.

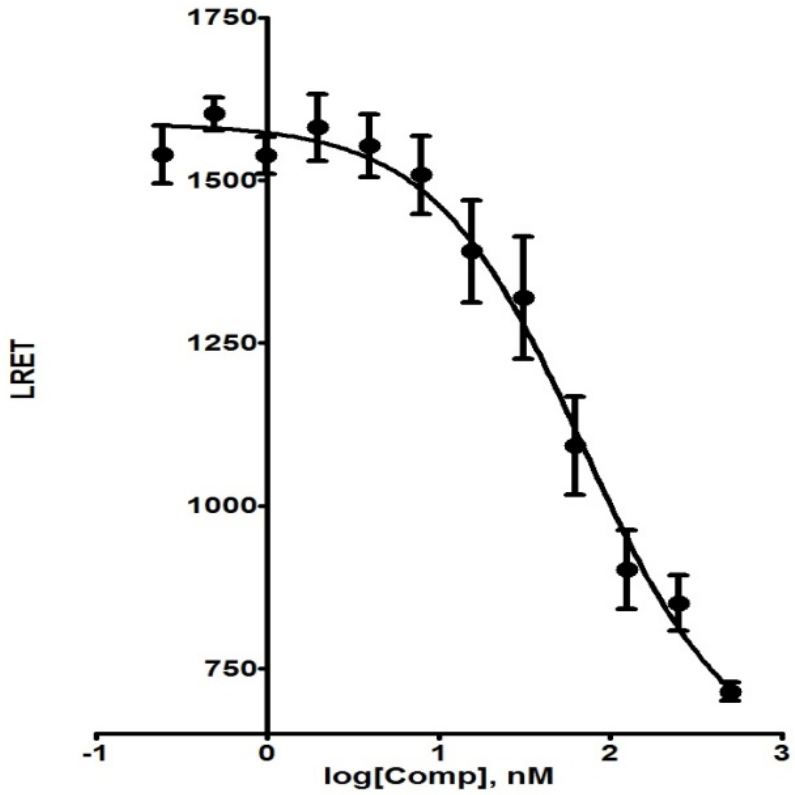

Figure 18: Intramolecular, luminescence resonance energy transfer (LRET) between pfDHFR-bound Tb^{3+} complex of MTX-TTHA-cs124 and GFP. Increasing concentrations of unlabeled Compound **1a** were titrated against a constant concentration (3 nM) of MTX TTHA cs124 Tb^{3+} and 30 nM of pfDHFR K27E-GFP. Sensitized GFP emission (520 nm) and Tb^{3+} emission (615 nm) was detected after a time delay of 100 μs, upon pulsed excitation with near-UV light (340 nm). The y-axis represents the GFP sensitized emission. Line represents nonlinear least-squares fit to the data

4.4 Conclusion

Antifolate lanthanide complexes demonstrated to be relatively stable under the presence of excess chelators. This characteristic was exploited to develop a method to measure binding affinities in cells lysates expressing a GFP-DHFR fusion protein. Given the unique photophysical characteristic of the lanthanide chelates and their relative stability, using antifolates conjugated to lanthanide complexes and DHFR to characterize binding affinity can be achieved with high signal to background ratio and accuracy under conditions where protein purification is difficult or impossible. The large dynamic range observed in the LRET binding assays suggest that this method can be applied to HTS assays.

A competitive binding assay using TR-LRET was developed. In this case, inhibitors of the DHFR for the malaria causing organism were analyzed. Displacement of antifolate Tb^{3+} complex (MTX-TTHA-cs124) is observed upon titration of an unlabeled antifolate. Inhibition constants were obtained from by non-linearly fitting the data. In the case of MTX inhibition, the measured inhibition constant closely matched the measured dissociation constant, suggesting this approach means of assessing enzyme:inhibitor binding affinities. A large dynamic range of LRET signal was also observed, which further suggests that this method may be applied to develop HTS assays. The possibility of developing a screening assay for inhibitors of drug-resistant forms of pfDHFR as well as additional applications of antifolate conjugates is explored in Chapter 5.

Chapter 5:

CONCLUSIONS AND FUTURE PERSPECTIVES

5.1 Introduction

In the previous chapters, methods were presented for the synthesis of substituted 5-benzyl pyrimidine antifolates and methotrexate that could be conjugated to fluorophores or other functional reporters without disrupting their DHFR-binding affinity. It was further shown that compounds **1a** and **2a** retained high selectivity and potency against their targets, pfDHFR and pcDHFR, respectively. Moreover, it was shown that conjugates of TMP and methotrexate linked to a luminescent terbium complex, TTHA-cs124, could be used as donors in luminescent resonance energy transfer (LRET) assays. This assay platform could be used to sensitively detect and quantify interactions (or inhibition of interaction) between the antifolate-terbium complex conjugates and GFP-DHFR fusion proteins by detecting terbium-to-GFP, LRET-sensitized emission in time-resolved mode. In this chapter, ongoing experiments that leverage these synthetic and biochemical results to develop new protein labeling reagents and high throughput (HTS) screening assays of ligand-protein and protein-protein interactions are discussed.

5.2 Future perspective

5.2.1 HTS malaria screening

TMP is a clinically validated therapy for malaria treatment. However, emergence of drug-resistant strains have limited its efficacy in recent years. Often, resistance to TMP therapy arises from expression of mutant forms of the DHFR enzyme that bind TMP with substantially lower affinity than the wild-type enzyme. For example, TMP is ~25-fold less potent against the commonly found resistant mutant pfDHFR (C59R S108N) and >500-fold less potent against the C59R S108N I164L mutation (37). Thus, there is a need for new antifolates that exhibit high potency against drug-resistant malaria DHFR while retaining high selectivity over mammalian

DHFR inhibition. Given this need, there have been efforts to develop HTS assays that could identify potential antifolates from compound libraries.

Several methods have been reported where identification of antifolates in high-throughput mode was assessed (64-67). However, these screens were either virtual (*in silico*), non-target-specific (cell-based), or not focused on pfDHFR. The only reported screen of pfDHFR entailed the immobilization of DHFR in a column follow by the addition of a mixture of inhibitors. After washing the column, bound molecules were eluted along with pfDHFR. Identification of the antifolates was performed by mass spectrometry (64). Even though this method can successfully identify inhibitors, its throughput does not correspond to a true HTS assay.

The sensitivity and robustness of TR-LRET has enabled HTS for antagonists/inhibitors of many targets including G-protein coupled receptors (GPCRs), kinases, ubiquitin, and protein-protein/peptide/DNA interactions (68). The usefulness of TR-LRET assays lies in their ability to eliminate non-specific fluorescence background signals from samples or compound libraries. In Chapter 4, it was shown that TR-LRET could be used to measure the inhibition constants of MTX and Compound **1a** against the purified, soluble domain of pfDHFR fused to GFP. The assay was straightforward, leveraging the high signal-to-background ratio detection of terbium-to-GFP LRET in 96-well plate format using a commercially available, time-resolved luminescence plate reader. The essential features of this approach, where inhibition is measured as the loss of LRET signal seen when an inhibitor reduces the binding of a MTX-terbium complex conjugate to pfDHFR-GFP, make it easily adaptable for HTS screening of compound libraries.

For HTS assays, one common measure of assay performance is Z'-factor:

$$Z' = 1 - \frac{(3\sigma_{max} + 3\sigma_{min})}{|\mu_{max} - \mu_{min}|} \quad (14)$$

calculated from the standard deviations and means of the maximum and minimum observed signal levels under controlled conditions (i.e., without library compounds present) (69). Z'-factor can vary between 0 and 1, with values >0.5 considered acceptable. We estimated the Z'-factor for **1a** inhibition of pfDHFR(K27E)-GFP from the highest and lowest observed signals seen in a competitive titration (Figure 19), obtaining an extremely high value of 0.7.

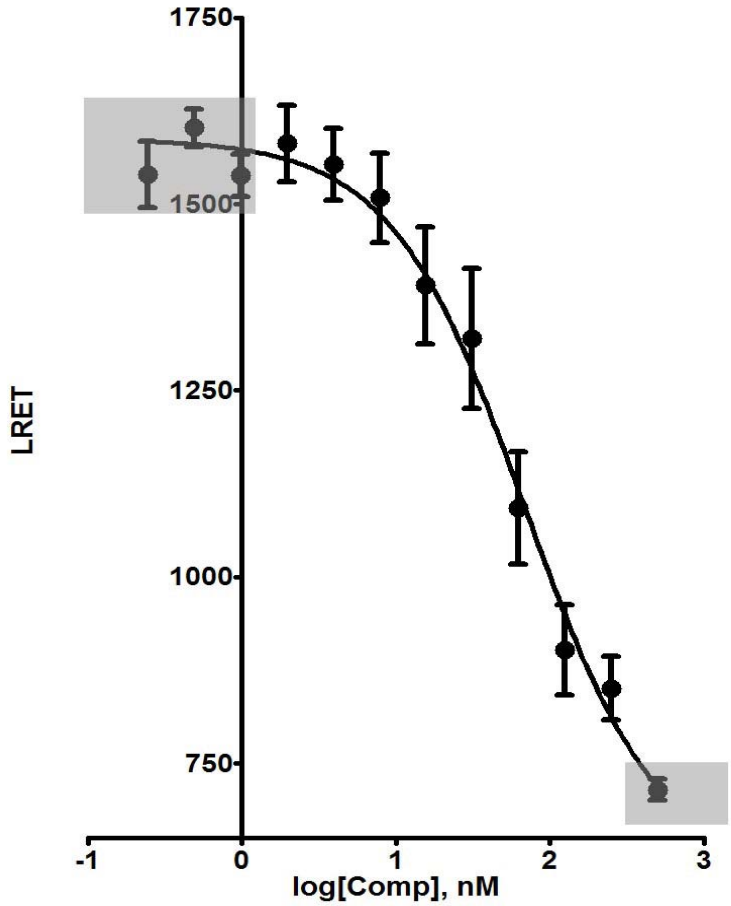

Figure 19:Calculation of Z' factor based in intramolecular, luminescence resonance energy transfer (LRET) between pfDHFR-bound Tb^{3+} complex of MTX-TTHA-cs124 and GFP. Increasing concentrations of unlabeled Compound **1a** were titrated against a constant concentration (3 nM) of MTX TTHA cs124 Tb^{3+} and 30 nM of pfDHFR K27E-GFP. Sensitized GFP emission (520 nm) and Tb^{3+} emission (615 nm) was detected after a time delay of 100 μs, upon pulsed excitation with near-UV light (340 nm). The y-axis represents the GFP sensitized emission. Line represents nonlinear least-squares fit to the data. Shadow represent points taken into consideration for Z' factor determination.

Given its sensitivity and accuracy, the TR-LRET assay platform can be extended to screen libraries for inhibitors of drug-resistant mutants of pfDHFR and subsequently quantify the inhibition constants of any identified lead compounds. Efforts to demonstrate this by testing the assay with purified GFP fusions of pfDHFR(K27E C59R S108N) are underway.

5.2.2 Characterization of protein-protein interactions with TR-LRET

Another feature of the antifolate-DHFR TR-LRET assay platform is its ability to directly quantify ligand-protein interactions directly in *E. coli* lysates that contain overexpressed GFP-DHFR fusion proteins, as was described in Chapter 4. In this case, GFP-DHFR fusions are overexpressed, and their concentration in lysates determined spectrophotmetrically. Then, antifolate-terbium complex conjugates are added directly to the lysates where they selectively label the proteins, and TR-LRET analysis can then be performed. The ability to label proteins in complex mixtures, and the kinetic stability of the terbium complexes is what enables this type of assay. These features point to the possibility of analyzing ligand-protein interactions or even protein-protein interactions in cases where purified protein preparations cannot be obtained.

Recently, protein-protein interaction analysis in bacterial lysates was demonstrated in the Miller laboratory. The interaction between FK506 binding protein 12 fused to GFP (GFP-FKBP) and the rapamycin-binding domain of mTor fused to eDHFR (FRB-eDHFR) was be sensitively detected and accurately quantified within an impure cell lysate matrix by LRET analysis following binding of TMP-TTHA-cs124(Tb^{3+}) to the fusion protein complex (Figure 20). These studies pave the way for ultimately detecting and measuring protein-protein interactions and their inhibition directly in live cells by using cell-permeable TMP-terbium complex conjugates to label overexpressed eDHFR fusions.

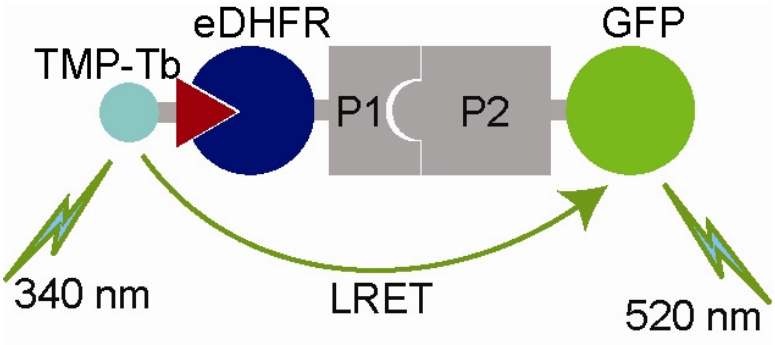

Figure 20. Schematic representation of LRET PPI assay mediated by trimethoprim (TMP)/*E. coli* dihydrofolate reductase (eDHFR) interaction. A TMP-Tb^{3+} complex conjugate binds specifically and tightly to eDHFR (K_D = ~2 nM). Interaction between eDHFR and GFP fusion proteins and excitation of TMP-Tb (the donor) results in LRET-sensitized emission of GFP (the acceptor).

5.2.3 Selective protein labeling and single molecule analysis

Single molecule imaging requires bright fluorophores that emit large numbers of photons before photobleaching. One limitation of live cell single molecule microscopy is the relatively poor brightness and photostability of fluorescent proteins relative to that seen with organic fluorophores such as Cy-5 or AlexaFluor 647. Certainly, protein labeling technologies should be amenable to labeling proteins in or on live cells with bright fluorophore-ligand conjugates. However, another factor that is important for single molecule studies is the stability of the fluorophore-protein complex. Because antifolate-DHFR interactions are non-covalent, the dissociation rate constant is equally important as the K_D for evaluating these systems as a potential means of labeling proteins for live cell single molecule imaging.

Using the synthetic methodologies presented in this dissertation, I and others in the Miller laboratory have prepared conjugates of tetramethylrhodamine (a common single molecule fluorophore) to 2,4-Diamino-5-(4'-methoxy)benzylpyrimidine, TMP, and MTX (Figure 21). Ensemble kinetic measurements for these antifolates have been reported giving dissociation rate constants of 0.27 s^{-1}, 0.01 s^{-1} and 0.0001 s^{-1}, respectively (70, 71). From these values, the expected half-lives of the respective antifolate-eDHFR complexes should range from seconds to hours. The efficacy of these compounds as single molecule protein labels is currently being evaluated.

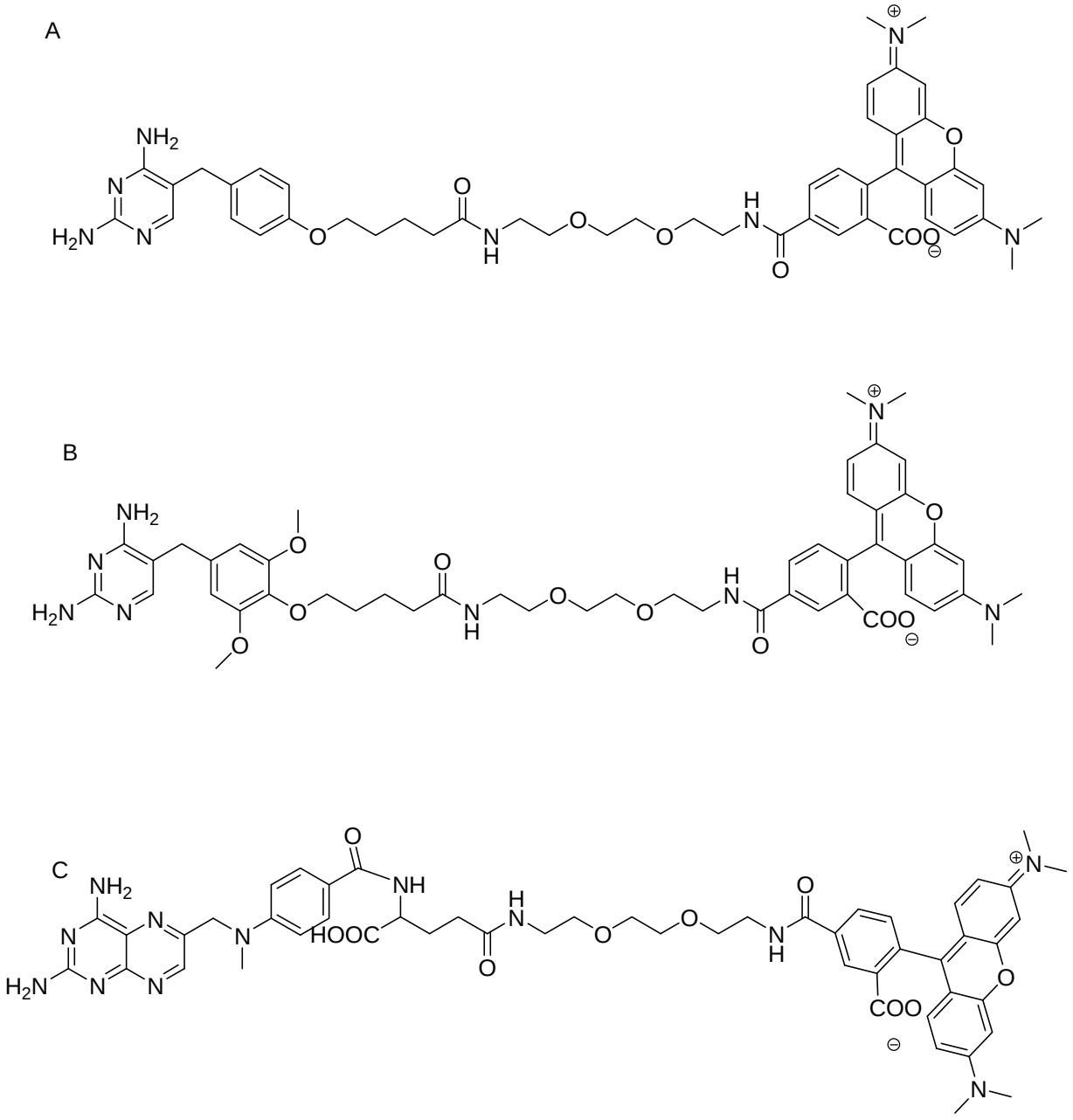

Figure 21: Tetramethylrhodamine conjugates of antifolates with a broad range of expected half-lives for binding to eDHFR, including (A) 2,4-Diamino-5-(4'-methoxy)benzylpyrimidine ($\tau_{1/2}$ = 2.5 s) (B) TMP ($\tau_{1/2}$ = 77 s) and (C) MTX ($\tau_{1/2}$ = 1.9 h). Synthesis of these analogs was enabled by the methodologies reported in this dissertation. The potential use of these conjugates for single molecule protein labeling and imaging studies is currently being evaluated.

5.3 General conclusions

Ligand-receptor interaction pairs that bind to one another with high selectivity and affinity can be used to develop a variety of tools and methods for live cell imaging, quantitative biochemical assays and HTS drug discovery efforts. The work presented in this dissertation sought to leverage the extensive medicinal chemistry efforts that have been devoted to finding highly selective and potent inhibitors of DHFRs from a variety of organisms. Biochemical analysis showed that inhibitors of pfDHFR and pcDHFR could be conjugated to fluorophores while retaining their target affinities. While efforts to label pfDHFR proteins in live mammalian cells were only marginally successful, it was shown that conjugates of a TMP and MTX could be coupled to a luminescent terbium complex and used for highly sensitive LRET assays of ligand-protein binding in buffer solution and in bacterial lysates. These assays should be adaptable to high-throughput detection formats, possibly enabling detection of novel DHFR inhibitors or even protein-protein interaction inhibitors in cases where purified proteins are difficult to obtain. Moreover, the synthetic methods used to prepare antifolate conjugates described here can be used to fine-tune the interactions between antifolate conjugates and their targets, potentially yielding effective methods of targeting proteins with single molecule detection-compatible fluorophores.

Chapter 6:

REFERENCES

1. Bucci M, Goodman C, Sheppard TL. 2010. *Nat Chem Biol* 6: 847-54

2. Schreiber SL. 1998. *Bioorg Med Chem* 6: 1127-52

3. Druker BJ, Talpaz M, Resta DJ, Peng B, Buchdunger E, et al. 2001. *N Engl J Med* 344: 1031-7

4. Lewis WG, Green LG, Grynszpan F, Radic Z, Carlier PR, et al. 2002. *Angew Chem Int Ed Engl* 41: 1053-7

5. Saxon E, Bertozzi CR. 2000. *Science* 287: 2007-10

6. McGinty RK, Kim J, Chatterjee C, Roeder RG, Muir TW. 2008. *Nature* 453: 812-6

7. Bishop A, Buzko O, Heyeck-Dumas S, Jung I, Kraybill B, et al. 2000. *Annu Rev Biophys Biomol Struct* 29: 577-606

8. Kiick KL, Saxon E, Tirrell DA, Bertozzi CR. 2002. *Proc Natl Acad Sci U S A* 99: 19-24

9. Prescher JA, Dube DH, Bertozzi CR. 2004. *Nature* 430: 873-7

10. Saxon E, Luchansky SJ, Hang HC, Yu C, Lee SC, Bertozzi CR. 2002. *J Am Chem Soc* 124: 14893-902

11. Bishop AC, Ubersax JA, Petsch DT, Matheos DP, Gray NS, et al. 2000. *Nature* 407: 395-401

12. Clackson T, Yang W, Rozamus LW, Hatada M, Amara JF, et al. 1998. *Proc Natl Acad Sci U S A* 95: 10437-42

13. Hwang YW, Miller DL. 1987. *J Biol Chem* 262: 13081-5

14. Tsien RY. 1998. *Annu Rev Biochem* 67: 509-44

15. Jing C, Cornish VW. 2011. *Acc Chem Res* 44: 784-92

16. Wombacher R, Cornish VW. 2011. *J Biophotonics* 4: 391-402

17. Adams SR, Campbell RE, Gross LA, Martin BR, Walkup GK, et al. 2002. *J Am Chem Soc* 124: 6063-76

18. Marek KW, Davis GW. 2002. *Neuron* 36: 805-13

19. Luedtke NW, Dexter RJ, Fried DB, Schepartz A. 2007. *Nat Chem Biol* 3: 779-84

20. Gaspersic J, Hafner-Bratkovic I, Stephan M, Veranic P, Bencina M, et al. 2010. *FEBS J* 277: 2038-50

21. Hu Y, Su B, Kim CS, Hernandez M, Rostagno A, et al. 2010. *Chembiochem* 11: 2409-18

22. Ignatova Z, Gierasch LM. 2004. *Proc Natl Acad Sci U S A* 101: 523-8

23. Ramdzan YM, Nisbet RM, Miller J, Finkbeiner S, Hill AF, Hatters DM. 2010. *Chem Biol* 17: 371-9

24. Stroffekova K, Proenza C, Beam KG. 2001. *Pflugers Arch* 442: 859-66

25. Keppler A, Gendreizig S, Gronemeyer T, Pick H, Vogel H, Johnsson K. 2003. *Nat Biotechnol* 21: 86-9

26. Keppler A, Pick H, Arrivoli C, Vogel H, Johnsson K. 2004. *Proc Natl Acad Sci U S A* 101: 9955-9

27. Farr GA, Hull M, Mellman I, Caplan MJ. 2009. *J Cell Biol* 186: 269-82

28. Kropf M, Rey G, Glauser L, Kulangara K, Johnsson K, Hirling H. 2008. *Eur J Cell Biol* 87: 763-78

29. Maurel D, Comps-Agrar L, Brock C, Rives ML, Bourrier E, et al. 2008. *Nat Methods* 5: 561-7

30. Marks KM, Rosinov M, Nolan GP. 2004. *Chem Biol* 11: 347-56

31. Rozinov MN, Nolan GP. 1998. *Chem Biol* 5: 713-28

32. Calloway NT, Choob M, Sanz A, Sheetz MP, Miller LW, Cornish VW. 2007. *Chembiochem* 8: 767-74

33. Miller LW, Cai Y, Sheetz MP, Cornish VW. 2005. *Nat Methods* 2: 255-7

34. Miller LW, Sable J, Goelet P, Sheetz MP, Cornish VW. 2004. *Angew Chem Int Ed Engl* 43: 1672-5

35. Rajapakse HE, Gahlaut N, Mohandessi S, Yu D, Turner JR, Miller LW. 2010. *Proc Natl Acad Sci U S A* 107: 13582-7

36. Cody V, Pace J, Chisum K, Rosowsky A. 2006. *Proteins* 65: 959-69

37. Kamchonwongpaisan S, Quarrell R, Charoensetakul N, Ponsinet R, Vilaivan T, et al. 2004. *J Med Chem* 47: 673-80

38. Rosowsky A, Forsch RA, Queener SF. 2002. *J Med Chem* 45: 233-41

39. Sirichaiwat C, Intaraudom C, Kamchonwongpaisan S, Vanichtanankul J, Thebtaranonth Y, Yuthavong Y. 2004. *J Med Chem* 47: 345-54

40. Blakley RL, Benkovic SJ. c1984. *Chemistry and biochemistry of folates*. New York: Wiley

41. Herbert V. *Annals of Internal Medicine* 72: 1/4p

42. Huennekens FM. 1996. *Protein Sci* 5: 1201-8

43. Farber S, Diamond LK. 1948. *N Engl J Med* 238: 787-93

44. Forsch RA, Queener SF, Rosowsky A. 2004. *Bioorg Med Chem Lett* 14: 1811-5

45. Yuvaniyama J, Chitnumsub P, Kamchonwongpaisan S, Vanichtanankul J, Sirawaraporn W, et al. 2003. *Nat Struct Biol* 10: 357-65

46. Japrung D, Chusacultanachai S, Yuvaniyama J, Wilairat P, Yuthavong Y. 2005. *Protein Eng Des Sel* 18: 457-64

47. Chusacultanachai S, Thiensathit P, Tarnchompoo B, Sirawaraporn W, Yuthavong Y. 2002. *Mol Biochem Parasitol* 120: 61-72

48. Sirawaraporn W, Sathitkul T, Sirawaraporn R, Yuthavong Y, Santi DV. 1997. *Proc Natl Acad Sci U S A* 94: 1124-9

49. Czlapinski JL, Schelle MW, Miller LW, Laughlin ST, Kohler JJ, et al. 2008. *J Am Chem Soc* 130: 13186-7

50. Gallagher SS, Miller LW, Cornish VW. 2007. *Anal Biochem* 363: 160-2

51. Rajapakse HE, Reddy DR, Mohandessi S, Butlin NG, Miller LW. 2009. *Angew Chem Int Ed Engl* 48: 4990-2

52. Reddy DR, Pedro Rosa LE, Miller LW. 2011. *Bioconjug Chem* 22: 1402-9

53. Hoskins AA, Friedman LJ, Gallagher SS, Crawford DJ, Anderson EG, et al. 2011. *Science* 331: 1289-95

54. Segel IH. 1975. *Enzyme kinetics : behavior and analysis of rapid equilibrium and steady state enzyme systems* New York: Wiley

55. Cheng Y, Prusoff WH. 1973. *Biochem Pharmacol* 22: 3099-108

56. Hanaoka K, Kikuchi K, Kobayashi S, Nagano T. 2007. *J Am Chem Soc* 129: 13502-9

57. Selvin PR, Hearst JE. 1994. *Proc Natl Acad Sci U S A* 91: 10024-8

58. Song B, Vandevyver CD, Chauvin AS, Bunzli JC. 2008. *Org Biomol Chem* 6: 4125-33

59. Kuyper LF, Roth B, Baccanari DP, Ferone R, Beddell CR, et al. 1982. *J Med Chem* 25: 1120-2

60. Rosowsky A, Cody V, Galitsky N, Fu H, Papoulis AT, Queener SF. 1999. *J Med Chem* 42: 4853-60

61. Tarnchompoo B, Sirichaiwat C, Phupong W, Intaraudom C, Sirawaraporn W, et al. 2002. *J Med Chem* 45: 1244-52

62. Sirawaraporn W, Prapunwattana P, Sirawaraporn R, Yuthavong Y, Santi DV. 1993. *J Biol Chem* 268: 21637-44

63. Selvin PR. 2002. *Annu Rev Biophys Biomol Struct* 31: 275-302

64. Thongpanchang C, Taweechai S, Kamchonwongpaisan S, Yuthavong Y, Thebtaranonth Y. 2007. *Anal Chem* 79: 5006-12

65. Dasgupta T, Chitnumsub P, Kamchonwongpaisan S, Maneeruttanarungroj C, Nichols SE, et al. 2009. *ACS Chem Biol* 4: 29-40

66. Plouffe D, Brinker A, McNamara C, Henson K, Kato N, et al. 2008. *Proc Natl Acad Sci U S A* 105: 9059-64

67. Zolli-Juran M, Cechetto JD, Hartlen R, Daigle DM, Brown ED. 2003. *Bioorg Med Chem Lett* 13: 2493-6

68. Degorce F, Card A, Soh S, Trinquet E, Knapik GP, Xie B. 2009. *Curr Chem Genomics* 3: 22-32

69. Inglese J, Johnson RL, Simeonov A, Xia M, Zheng W, et al. 2007. *Nat Chem Biol* 3: 466-79

70. Baccanari DP, Daluge S, King RW. 1982. *Biochemistry* 21: 5068-75

71. Appleman JR, Howell EE, Kraut J, Kuhl M, Blakley RL. 1988. *J Biol Chem* 263: 9187-98

Chapter 7

VITA

Name: **Laura E. Pedró Rosa**

Education: University of Puerto Rico-Rio Piedras Chemistry, BS, 2006

Protessional Experience

2006-Present	Graduate Research Assistant, University of Illinois at Chicago, Il.
2008-2010	Teaching Assistant, University of Illinois at Chicago, Il.
2006	Research Assistant, Materials Characterization Center, San Juan, P.R.
2005	Summer Intern, Northwestern University, Evanston, Il.
2004-2005	Undergraduate Research Assistant, University of Puerto Rico-RP, P.R.
2004	Summer Intern, Autoridad de Energia Electrica, San Juan, P.R.

Publications

1. **Pedró Rosa**, **L.E.,** Miller, L.W. "Modulating the kinetics of antifolate-dihydroflate reductase interactions for chemical protein labeling applications." *In preparation*, 2011.
2. Reddy, D.R., **Pedró Rosa**, **L.E.,** Miller, L.W. "Luminescent trimethoprim-polyaminocarboxylate lanthanide complex conjugates for selective protein labeling and time-resolved bioassays." *Bioconjugate Chemistry*. *In Press*, 2011.
3. **Pedró Rosa, L.E.**, Reddy, D.R., Queener, S.F., Miller, L.W. "Selective antifolates for labeling proteins in mammalian cells." *ChemBioChem.* 2009, 10, 1462-1464.
4. Cardona, R. A., Hernández, K., **Pedró, L.E.**, Otaño, M.R., Montes, I. , Guadalupe, A.R.. "Electrochemical and Spectroscopical of Ferrocenyl Chalcones." *Journal of the Electrochemical Society*. 2010, 157, F104-F110.

Presentations

1. NSF 2010 JAM. Student Panel. June 6-9, 2010. Washington D.C
2. Bioorganic Gordon Research Conference. Selective antifolates for chemically labeling proteins inside the cell. June 14-19th, 2009. Andover, NH
3. IAHLEA Research Forum. In-Vivo protein labeling with antifolate derivatives. April 24, 2008. Chicago, IL.
4. 2007 IL-LSAMP Regional Conference. In-Vivo protein labeling with antifolate derivatives. October 12-13, 2007. Glenview, IL